

On Migdal's theorem and the pseudogap

P. Monthoux

Cavendish Laboratory, University of Cambridge

Madingley Road, Cambridge CB3 0HE, United Kingdom

(October 29, 2018)

Abstract

We study a model of quasiparticles on a two-dimensional square lattice coupled to Gaussian distributed dynamical molecular fields. We consider two types of such fields, a vector molecular field that couples to the quasiparticle spin-density and a scalar field coupled to the quasiparticle number density. The model describes quasiparticles coupled to spin or charge fluctuations, and is solved by a Monte Carlo sampling of the molecular field distributions. When the molecular field correlations are sufficiently weak, the corrections to the self-consistent Eliashberg theory do not bring about qualitative changes in the quasiparticle spectrum. But for a range of model parameters near the magnetic boundary, we find that Migdal's theorem does not apply and the quasiparticle spectrum is qualitatively different from its Eliashberg approximation. In the range of model parameters studied, we find the transverse spin-fluctuation modes play a key role. While a pseudogap opens when quasiparticles are coupled to antiferromagnetic fluctuations, such a pseudogap is not observed in the corresponding charge-fluctuation case for the range of parameters studied, where vertex corrections are found to effectively reduce the strength of the interaction. This suggests that one has to be closer to the border of long-range order to observe pseudogap effects in the charge-fluctuation

case than for a spin-fluctuation induced interaction under otherwise similar conditions.

An important feature of the magnetic pseudogap found in the present calculations is that it is strongly anisotropic. It vanishes along the diagonal of the Brillouin zone and is large near the zone boundary. In the case of ferromagnetic fluctuations, we also find a range of model parameters with qualitative changes in the quasiparticle spectral function not captured by the one-loop approximation, in that the quasiparticle peak splits into two. We find that one needs to be closer to the magnetic boundary to observe the pseudogap effects in the nearly ferromagnetic case relative to the nearly antiferromagnetic one, under otherwise similar conditions. We provide intuitive arguments to explain the physical origin of the breakdown of Migdal's theorem.

PACS Nos. 71.27.+a

I. INTRODUCTION

The polarizer-analyser analogy provides an intuitive description of the effective interaction between quasiparticles in a quantum many-body system. The first quasiparticle polarizes the medium in which it travels and the second quasiparticle, the analyser, feels the disturbance induced by the first one. In a strongly correlated system one can expect this induced polarization of the medium to be very complex, and in practice simplifying assumptions are made. A commonly used approximation is the description of the polarization effects by the appropriate linear response function of the material. Furthermore, one typically only considers the interaction channel for which the linear response of the system is the largest. On the border of long-range magnetic order for instance, the spin-spin correlation function is the most enhanced and it is plausible that the dominant interaction channel is of magnetic origin and depends on the relative spin orientations of the interacting quasiparticles.

It has been shown that such a magnetic interaction, treated in the self-consistent Eliashberg approximation, can produce anomalous normal state properties and superconducting instabilities to anisotropic pairing states. It correctly predicted the symmetry of the Cooper state in the copper oxide superconductors [1] and is consistent with spin-triplet p-wave pairing in superfluid ^3He [for a recent review see, e.g., Ref. [2]]. One also gets the correct order of magnitude of the superconducting and superfluid transition temperature T_c when the model parameters are inferred from experiments in the normal state of the above systems. For the case of a nearly half-filled single band, the calculations showed that the Eliashberg superconducting transition temperature T_c is higher for the tetragonal (quasi-2D) than cubic (3D) lattice [3–6]. Particularly striking is the comparison between the cubic antiferromagnetic metal CeIn_3 and the closely related compound CeCoIn_5 [7]. Superconductivity is found to extend over a much wider range in both temperature and pressure in CeCoIn_5 than in CeIn_3 . These findings and the growing evidence that the pairing symmetry in CeCoIn_5 is d-wave in character, were correctly anticipated by the magnetic interaction model.

While there have been a number of examples of superconductivity on the border of anti-

ferromagnetism, the corresponding phenomenon on the edge of metallic ferromagnetism has only been found recently. This result is not surprising within the framework of the magnetic interaction model. For otherwise equivalent conditions, the superconducting transition temperature is typically much higher on the border of antiferromagnetism than on the border of ferromagnetism [5,6,8]. An intuitive understanding of this finding pointed to candidate systems in which superconductivity on the border of ferromagnetism would be more likely to be observed. In particular, one ought to look for systems with strong spin anisotropy, i.e, with strong spin-orbit coupling and/or in a weakly spin-polarized state. This suggested a more detailed investigation of UGe_2 at high pressure which satisfied the above conditions and could be prepared in high purity form. This material proved to be the first example of the co-existence of superconductivity and itinerant-electron ferromagnetism [9].

The self-consistent Eliashberg treatment of the magnetic interaction model can produce strongly damped quasiparticles, but the electronic spectral function one obtains always shows a quasiparticle peak as one approaches the Fermi level. This is in qualitative disagreement with photoemission experiments on underdoped cuprate superconductors which show a near absence of a quasiparticle peak near the $(\pi, 0)$ point in the Brillouin zone [10]. This depletion of quasiparticle states, or pseudogap, is also seen in thermodynamic measurements [11]. The phenomenon may not be specific to the underdoped cuprates. For instance, the possible existence of a pseudogap in the heavy fermion compound $CeCoIn_5$ has recently been reported [12].

Is the disagreement between theory and experiment the manifestation of a fundamental flaw in the approach or does it simply reflect the inadequacy of the approximations used in the solution of the model? Questions regarding the validity of the Eliashberg treatment of the magnetic interaction model have been raised [13]. The one-loop approximation effectively assumes that quasiparticles behave as test particles. There must therefore be corrections to the simple theory, referred to as vertex corrections, coming from the fact that real and test particles behave differently. One can expect these vertex corrections to produce quantitative changes to the self-consistent Eliashberg theory as one approaches the border of long-range

magnetic order. In Ref. [14] it was shown that for optimally doped cuprates, vertex corrections did not bring about significant changes to the single spin-fluctuation approximation, producing an enhancement of the spin-fluctuation interaction of the order of 20%. The sign of this correction [14] is opposite to that expected in the case of a phonon-mediated interaction [15] and in the spin-density-wave phase [13]. This enhancement of the fermion spin-fluctuation vertex in the paramagnetic state is due to the transverse spin-fluctuation modes.

It has been argued, in particular by Schrieffer [13], that as the antiferromagnetic correlations get stronger, the system should display characteristics akin to the antiferromagnetic insulating state and that the behavior of the quasiparticles should become qualitatively different from that of a simple metal. The results presented here show that this physical insight is correct in that Migdal's theorem can qualitatively break down when the antiferromagnetic correlations become strong enough and a different state emerges.

The validity of Baym-Kadanoff many-body theories such as the fluctuation exchange approximation [16], which is in many ways similar to the Eliashberg theory of the magnetic interaction model, has been extensively studied by Tremblay and collaborators in the context of the Hubbard model [17–19]. They find that close to the magnetic boundary, Migdal's theorem qualitatively breaks down, in that a critical-fluctuation-induced pseudogap (or precursor pseudogap) is observed in the Quantum Monte Carlo simulations but is not found in the fluctuation exchange approximation. Similar results about the role of vertex corrections were reported in the case of the attractive Hubbard model [20–24], where in this case the precursor pseudogap is caused by critical pairing fluctuations.

In this paper, we examine corrections to the single spin-fluctuation exchange approximation in two dimensions using a non-perturbative formulation of the magnetic interaction model which is amenable to computer simulation [25]. We find that as the antiferromagnetic correlations become strong enough for vertex corrections to produce a qualitative change relative to the one-loop approximation, a pseudogap opens in the quasiparticle spectrum. In this respect, our results are similar to those obtained for the Hubbard model [17–19]. The

pseudogap we find is strongly anisotropic in that it vanishes along the diagonal of the Brillouin zone and is large near the zone boundary. We demonstrate that, in the range of model parameters studied here, the transverse spin-fluctuation modes are key to the appearance of the pseudogap by considering the case of commensurate charge-fluctuations with a spectrum identical to that of the paramagnons. While a pseudogap opens when quasiparticles are coupled to magnetic fluctuations, such a pseudogap is not observed in the corresponding charge-fluctuation case for the range of parameters studied, where vertex corrections are found to effectively reduce the strength of the interaction. This suggests that one has to be closer to the border of long-range order to observe pseudogap effects in the charge-fluctuation case than for a spin-fluctuation induced interaction under otherwise similar conditions. In the case of nearly ferromagnetic systems, as magnetic correlations get stronger, we also find qualitative changes in the quasiparticle spectral function not captured by the one-loop approximation. The quasiparticle peak splits into two distinct peaks with a lowering of the tunneling density of states at the Fermi level. For the range of parameters studied, this suppression of the tunneling density of states at the Fermi level is weaker than in the case of nearly antiferromagnetic systems for otherwise similar magnetic and electronic spectrum parameters.

The paper is organized as follows. In the next section we describe the model and the class of vertex corrections considered. Section III contains the results of the numerical simulations. In section IV, we give intuitive arguments for the physical origin of the pseudogap. Finally we give a summary and outlook. Most of the technical details are included in an appendix.

II. MODEL

There are essentially two different ways to describe quantum many-body systems. In the Newtonian or Hamiltonian approach, one considers particles interacting with each other via pairwise interaction potentials. This is the point of view commonly adopted in the perturbation-theoretic approach to the non-relativistic many-electron problem. In the rela-

tivistic version of the theory, however, one adopts a Maxwellian point of view in which the interactions between electrons are mediated by a field, the quantized electromagnetic field. The Maxwellian approach is also widely used to carry out numerical simulations of interacting systems based on the Feynman path integral. In such functional integrals, bosonic fields are represented by c-numbers. But fermion fields must be represented by anticommuting, or Grassmann, numbers that are not easily handled by digital computers. When a dynamical molecular (or Hubbard-Stratonovich) field is introduced to mediate the interactions between the fermions, the problem is reduced to that of non-interacting particles in a fluctuating field. The integrals over the anticommuting variables can then be evaluated exactly, at least formally, thus eliminating the troublesome Grassmann numbers from the problem. In the following, we adopt the Maxwellian point of view and use dynamical molecular fields to mediate the interactions between quasiparticles.

In general, the distribution of Hubbard-Stratonovich fields is very complex and usually leads to intractable problems due to the infamous "fermion sign problem". In a many-body system, the presence of other particles produces changes in the effective interaction between two particles through screening effects and induces arbitrarily complex self-interactions of the dynamical molecular fields.

In this paper, we assume that the renormalization of the effective two-body interaction can be accounted for by a redefinition of the parameters entering the bare interaction. And we ignore all the self-interactions of the Hubbard-Stratonovich fields. The model was introduced in Ref. [25] and bears some resemblance to the "quenched approximation" of lattice gauge theories introduced by Marinari et al., who, incidentally, chose the name by analogy to condensed matter physics [26]. A recent application of the quenched approximation to the pseudogap problem for static Hubbard-Stratonovich fields and a clear exposition of the formalism is given by Posazhennikova and Coleman [27]. But in the present work, however, we use dynamical rather than static Hubbard-Stratonovich fields and a non-separable form of the molecular field correlation function.

Very close to the boundary of magnetic or charge long-range order, the self-interactions

of the dynamical molecular field ignored in the present work are known to be important for low dimensional systems [28]. The approximations made here may not be appropriate in a number of other cases. The virtue of the present approach is that it gives insights into quantum many-body problems that are essentially non-perturbative. More importantly, the results presented in this paper demonstrates that the simplest model already yields interesting physics. Some of the simplifications made here can in principle be relaxed and the theory extended accordingly.

To be more specific, we consider particles on a two-dimensional square lattice whose Hamiltonian in the absence of interactions is

$$\hat{h}_0(\tau) = - \sum_{i,j,\alpha} t_{ij} \psi_{i\alpha}^\dagger(\tau) \psi_{j\alpha}(\tau) - \mu \sum_{i\alpha} \psi_{i\alpha}^\dagger(\tau) \psi_{i\alpha}(\tau) \quad (2.1)$$

where t_{ij} is the tight-binding hopping matrix, μ the chemical potential and $\psi_{i\alpha}^\dagger$, $\psi_{i\alpha}$ respectively create and annihilate a fermion of spin orientation α at site i . We take $t_{ij} = t$ if sites i and j are nearest-neighbors and $t_{ij} = t'$ if sites i and j are next-nearest-neighbors.

To introduce interactions between the particles, we couple them to a dynamical molecular (or Hubbard-Stratonovich) field. It is instructive to consider two different types of molecular fields. In the first instance, we consider a vector Hubbard-Stratonovich field that couples locally to the fermion spin density. This is the case considered in Ref. [25] and describes quasiparticles coupled to magnetic fluctuations. To illustrate the role played by transverse spin-fluctuations we shall also consider the case of a scalar field that couples locally to the fermion number density. This case corresponds to a coupling to charge-fluctuations or, within the approximation we are using here, "Ising"-like magnetic fluctuations where only longitudinal modes are present. The Hamiltonians at imaginary time τ for particles coupled to the fluctuating exchange or scalar dynamical field are then

$$\hat{h}(\tau) = \hat{h}_0(\tau) - \frac{g}{\sqrt{3}} \sum_{i\alpha\gamma} \mathbf{M}_i(\tau) \cdot \psi_{i\alpha}^\dagger(\tau) \boldsymbol{\sigma}_{\alpha\gamma} \psi_{i\gamma}(\tau) \quad (2.2)$$

$$\hat{h}(\tau) = \hat{h}_0(\tau) - g \sum_{i\alpha} \Phi_i(\tau) \psi_{i\alpha}^\dagger(\tau) \psi_{i\alpha}(\tau) \quad (2.3)$$

where $\mathbf{M}_i(\tau) = (M_i^x(\tau), M_i^y(\tau), M_i^z(\tau))^T$ and $\Phi_i(\tau)$ are the real vector exchange and scalar

Hubbard-Stratonovich fields respectively, and g the coupling constant. The reason for the choice of an extra factor $1/\sqrt{3}$ in Eq. (2.2) will become clear later.

Since we ignore the self-interactions of the molecular fields, their distribution is Gaussian and given by [25]

$$\mathcal{P}[\mathbf{M}] = \frac{1}{Z} \exp \left(- \sum_{\mathbf{q}, \nu_n} \frac{\mathbf{M}(\mathbf{q}, i\nu_n) \cdot \mathbf{M}(-\mathbf{q}, -i\nu_n)}{2\alpha(\mathbf{q}, i\nu_n)} \right) \quad (2.4)$$

$$Z = \int D\mathbf{M} \exp \left(- \sum_{\mathbf{q}, \nu_n} \frac{\mathbf{M}(\mathbf{q}, i\nu_n) \cdot \mathbf{M}(-\mathbf{q}, -i\nu_n)}{2\alpha(\mathbf{q}, i\nu_n)} \right) \quad (2.5)$$

in the case of a vector exchange molecular field and

$$\mathcal{P}[\Phi] = \frac{1}{Z} \exp \left(- \sum_{\mathbf{q}, \nu_n} \frac{\Phi(\mathbf{q}, i\nu_n) \Phi(-\mathbf{q}, -i\nu_n)}{2\alpha(\mathbf{q}, i\nu_n)} \right) \quad (2.6)$$

$$Z = \int D\Phi \exp \left(- \sum_{\mathbf{q}, \nu_n} \frac{\Phi(\mathbf{q}, i\nu_n) \Phi(-\mathbf{q}, -i\nu_n)}{2\alpha(\mathbf{q}, i\nu_n)} \right) \quad (2.7)$$

in the case of a scalar Hubbard-Stratonovich field. In both cases $\nu_n = 2\pi nT$ since the dynamical molecular fields are periodic functions in the interval $[0, \beta = 1/T]$. The Fourier transforms of the molecular fields are defined as

$$\mathbf{M}_{\mathbf{R}}(\tau) = \sum_{\mathbf{q}, \nu_n} \mathbf{M}(\mathbf{q}, i\nu_n) \exp \left(-i[\mathbf{q} \cdot \mathbf{R} - \nu_n \tau] \right) \quad (2.8)$$

$$\Phi_{\mathbf{R}}(\tau) = \sum_{\mathbf{q}, \nu_n} \Phi(\mathbf{q}, i\nu_n) \exp \left(-i[\mathbf{q} \cdot \mathbf{R} - \nu_n \tau] \right) \quad (2.9)$$

We are considering the case where there is no long-range magnetic or charge order. The average of the dynamical molecular fields must then vanish and their Gaussian distributions Eqs. (2.4,2.6) are completely determined by their variance $\alpha(\mathbf{q}, i\nu_n)$, which we take to be

$$\alpha(\mathbf{q}, i\nu_n) = \begin{cases} \frac{1}{2} \frac{T}{N} \chi(\mathbf{q}, i\nu_n) & \text{if } \mathbf{M}(\mathbf{q}, i\nu_n) \text{ or } \Phi(\mathbf{q}, i\nu_n) \text{ complex} \\ \frac{T}{N} \chi(\mathbf{q}, i\nu_n) & \text{if } \mathbf{M}(\mathbf{q}, i\nu_n) \text{ or } \Phi(\mathbf{q}, i\nu_n) \text{ real} \end{cases} \quad (2.10)$$

where N is the number of allowed wavevectors in the Brillouin zone. Then

$$\langle M_i(\mathbf{q}, i\nu_n) M_j(\mathbf{k}, i\Omega_n) \rangle = \frac{T}{N} \chi(\mathbf{q}, i\nu_n) \delta_{\mathbf{q}, -\mathbf{k}} \delta_{\nu_n, -\Omega_n} \delta_{i,j} \quad (2.11)$$

$$\langle \Phi(\mathbf{q}, i\nu_n) \Phi(\mathbf{k}, i\Omega_n) \rangle = \frac{T}{N} \chi(\mathbf{q}, i\nu_n) \delta_{\mathbf{q}, -\mathbf{k}} \delta_{\nu_n, -\Omega_n} \quad (2.12)$$

where $\langle \dots \rangle$ denotes an average over the probability distributions Eq. (2.4) and Eq. (2.6) for the vector and scalar cases respectively. In order to compare the scalar and vector molecular fields, we take the same form for their correlation function $\chi(\mathbf{q}, i\nu_n)$ and parametrize it as in Refs. [5,8]. In what follows, we set the lattice spacing a to unity. For real frequencies, we have

$$\chi(\mathbf{q}, \omega) = \frac{\chi_0 \kappa_0^2}{\kappa^2 + \hat{q}^2 - i \frac{\omega}{\eta(\hat{q})}} \quad (2.13)$$

where κ and κ_0 are the correlation wavevectors or inverse correlation lengths in units of the lattice spacing, with and without strong correlations, respectively. Let

$$\hat{q}_\pm^2 = 4 \pm 2(\cos(q_x) + \cos(q_y)) \quad (2.14)$$

We shall consider commensurate charge-fluctuations and antiferromagnetic spin-fluctuations, in which case the parameters \hat{q}^2 and $\eta(\hat{q})$ in Eq. (2.13) are defined as

$$\hat{q}^2 = \hat{q}_+^2 \quad (2.15)$$

$$\eta(\hat{q}) = T_0 \hat{q}_- \quad (2.16)$$

where T_0 is a characteristic temperature.

We shall also consider the case of ferromagnetic spin-fluctuations, where the parameters \hat{q}^2 and $\eta(\hat{q})$ in Eq. (2.13) are given by

$$\hat{q}^2 = \hat{q}_-^2 \quad (2.17)$$

$$\eta(\hat{q}) = T_0 \hat{q}_- \quad (2.18)$$

$\chi(\mathbf{q}, i\nu_n)$ is related to the imaginary part of the response function $Im\chi(\mathbf{q}, \omega)$, Eq. (2.13), via the spectral representation

$$\chi(\mathbf{q}, i\nu_n) = - \int_{-\infty}^{+\infty} \frac{d\omega}{\pi} \frac{Im\chi(\mathbf{q}, \omega)}{i\nu_n - \omega} \quad (2.19)$$

To get $\chi(\mathbf{q}, i\nu_n)$ to decay as $1/\nu_n^2$ as $\nu_n \rightarrow \infty$, as it should, we introduce a cutoff ω_0 and take $Im\chi(\mathbf{q}, \omega) = 0$ for $\omega \geq \omega_0$. A natural choice for the cutoff is $\omega_0 = \eta(\hat{q})\kappa_0^2$.

In the approximation we are considering, the single particle Green's function is the average over the probability distributions $\mathcal{P}[\mathbf{M}]$ (Eq. (2.4)) or $\mathcal{P}[\Phi]$ (Eq. (2.6)) of the fermion Green's function in a dynamical vector or scalar field.

$$\mathcal{G}(i\sigma\tau; j\sigma'\tau') = \int D\mathbf{M} \mathcal{P}[\mathbf{M}] G(i\sigma\tau; j\sigma'\tau'|[\mathbf{M}]) \quad (2.20)$$

$$\mathcal{G}(i\sigma\tau; j\sigma'\tau') = \int D\Phi \mathcal{P}[\Phi] G(i\sigma\tau; j\sigma'\tau'|[\Phi]) \quad (2.21)$$

where

$$G(i\sigma\tau; j\sigma'\tau'|[\mathbf{M}] \text{ or } [\Phi]) = -\langle T_\tau \{ \psi_{i\sigma}(\tau) \psi_{j\sigma'}^\dagger(\tau') \} \rangle \quad (2.22)$$

is the single particle Green's function in a dynamical molecular field and is discussed in the appendix. In evaluating expressions Eqs. (2.20,2.21) one is summing over all Feynman diagrams corresponding to spin or charge-fluctuation exchanges [25,27]. The diagrammatic expansion of the Green's function in a dynamical field, Eq. (2.22) and its average, Eq. (2.20) are shown pictorially in Fig. 1. A non-perturbative study of quasiparticles coupled to static magnetic fluctuations using a diagram summation technique was reported in Ref. [29]. In this paper we do not resort to a diagrammatic expansion but rather evaluate the averages in Eqs. (2.20,2.21) over the dynamical molecular fields by Monte Carlo sampling.

It is very instructive to compare the results of the Monte Carlo simulations with the self-consistent Eliashberg calculations for the same model. If one only considers single spin or charge-fluctuation exchange processes, the single particle Green's function is given by:

$$\Sigma(\mathbf{p}, i\omega_n) = g^2 \frac{T}{N} \sum_{\Omega_n} \sum_{\mathbf{k}} \chi(\mathbf{p} - \mathbf{k}, i\omega_n - i\Omega_n) \mathcal{G}(\mathbf{k}, i\Omega_n) \quad (2.23)$$

$$\mathcal{G}(\mathbf{p}, i\omega_n) = \frac{1}{i\omega_n - (\epsilon_{\mathbf{p}} - \mu) - \Sigma(\mathbf{p}, i\omega_n)} \quad (2.24)$$

where $\Sigma(\mathbf{p}, i\omega_n)$ is the quasiparticle self-energy, $\mathcal{G}(\mathbf{p}, i\omega_n)$ the one-particle Green's function. $\epsilon_{\mathbf{p}}$ is the tight-binding dispersion relation obtained from Fourier transforming the hopping matrix t_{ij} in Eq. (2.1) and μ the chemical potential. The choice of the factor $1/\sqrt{3}$ in Eq. (2.2) means one obtains the same one-loop equations in the the case of an exchange molecular

field \mathbf{M} and that of the scalar field Φ , thereby simplifying the comparison between the two cases.

III. RESULTS

The quasiparticle dispersion relation for the two-dimensional square lattice is obtained from Eq. (2.1). We measure all energies and temperatures in units of the nearest-neighbor hopping parameter t . We set the next-nearest-neighbor hopping parameter $t' = -0.45t$. The chemical potential is adjusted so that the electronic band filling is $n = 0.9$. The dimensionless parameters describing the molecular field correlations are $g^2\chi_0/t$, T_0/t , κ_0 and κ . A complete exploration of the parameter space of the model is beyond the scope of this preliminary study. We chose a representative value for $\kappa_0^2 = 12$, and set $T_0 = 0.67t$ as in our earlier work [5,8]. For an electronic bandwidth of $1eV$, $T_0 \approx 1000^\circ K$. We only consider one value of the coupling constant $g^2\chi_0/t = 2$. In the random phase approximation, the magnetic instability would be obtained for a value of $g^2\chi_0/t$ of the order of 10. We consider what happens to the quasiparticle spectrum at a fixed temperature $T = 0.25t$ as the inverse correlation length κ changes.

The calculations were done on a 16 by 16 lattice, with 41 imaginary time slices, or equivalently 41 Matsubara frequencies for the molecular fields, $\mathbf{M}(\mathbf{q}, i\nu_n)$ and $\Phi(\mathbf{q}, i\nu_n)$ ($\nu_n = 2\pi nT$, with $n = 0, \pm 1, \dots, \pm 20$).

By analytic continuation of the single particle Green's function $\mathcal{G}(\mathbf{k}, \tau)$ or $\mathcal{G}(\mathbf{k}, i\omega_n)$ one can obtain the quasiparticle spectral function $A(\mathbf{k}, \omega) = -\frac{1}{\pi} \text{Im} \mathcal{G}_R(\mathbf{k}, \omega)$ and the tunneling density of states $N(\omega) = \frac{1}{N} \sum_{\mathbf{k}} A(\mathbf{k}, \omega)$, where $\mathcal{G}_R(\mathbf{k}, \omega)$ is the retarded single particle Green's function. In the case of the one-loop approximation, $\mathcal{G}(\mathbf{k}, i\omega_n)$ is analytically continued from imaginary to real frequencies by means of Padé approximants [30]. The imaginary time Monte Carlo data is analytically continued with the Maximum Entropy method [31]. We have used 2000 MC samples binned in groups of 20 to make 100 measurements. We have used three different versions of the Maximum Entropy method. The Classic MaxEnt and

two versions of Average MaxEnt, which is the method recommended in Ref. [31], where the probability for the α parameter is either a constant or proportional to $1/\alpha$ [31]. In all cases we chose a flat default model. The results for the three different versions of the Maximum Entropy method tried were nearly identical in the case of the vector molecular field. There were slight differences between the Classic and Average MaxEnt solutions for the spectral function in the scalar molecular field case, while the two versions of the Average MaxEnt gave nearly identical results. The choice of the $\sim 1/\alpha$ probability distribution in the Average MaxEnt method gave a slightly better fit to the MC data and all the results shown here are those obtained with this choice of probability distribution for the α parameter.

Fig. 2 shows the tunneling density of states $N(\omega)$ and the spectral function $A(\mathbf{k}, \omega) = -\frac{1}{\pi} \text{Im} \mathcal{G}_R(\mathbf{k}, \omega)$ for the one-loop Eliashberg approximation to the Green's function, Eqs. (2.23, 2.24), in the case of commensurate charge-fluctuations and antiferromagnetic spin-fluctuations. Figs. 2b,c show a strong anisotropy of the spectral function. $A(\mathbf{k}, \omega)$ is sharper when \mathbf{k} is along the diagonal compared to the case where \mathbf{k} is near a hot spot (which is a point on the Fermi surface accessible from another via a momentum transfer of $\mathbf{Q} = (\pi, \pi)$). Also note the monotonic broadening of $A(\mathbf{k}, \omega)$ as the parameter κ^2 is reduced.

In Fig. 3 we show the tunneling density of states and quasiparticle spectral function one obtains from the Monte Carlo calculation with a coupling to the scalar dynamical molecular field Φ . By comparison to the one-loop self-consistent results of Fig. 2, the vertex corrections give rise to a sharpening of the quasiparticle spectral function, except for $\kappa^2 = 4$ and $\mathbf{k} = (3\pi/8, 3\pi/8)$. For the range of values of model parameters considered here, the multiple charge-fluctuation exchanges do not lead to a breakdown of the quasiparticle picture. Note that contrary to the Eliashberg result, as κ^2 is reduced from 4, the spectral function initially sharpens before broadening again at the lower values of κ^2 considered here. For $\kappa^2 = 4, 2$, the spectral function is sharper near the hot spot than along the diagonal, again in contrast to the one-loop self-consistent result. It is approximately isotropic at $\kappa^2 = 1$ and becomes sharper along the diagonal than near the hot spot at the lower values of $\kappa^2 = 0.50, 0.25$. Quite generally Fig. 3 shows that when vertex corrections are included the spectral function

is less anisotropic than the Eliashberg result for the values of κ^2 considered.

The Monte Carlo results for quasiparticles coupled to antiferromagnetic spin-fluctuations are shown in Fig. 4. For $\kappa^2 \leq 1$, a pseudogap appears at the point $\mathbf{k} = (\pi, \pi/8)$ but not along the diagonal, in qualitative agreement with experiments on underdoped cuprates [10]. The pseudogap also shows up in the tunneling density of states $N(\omega)$ which is suppressed at the Fermi level for $\kappa^2 \leq 1$. By comparing the spectral function of Figs. 4b,c to the one-loop self-consistent result, we see that for the values of κ^2 where there isn't a pseudogap, vertex corrections lead to a broadening of the spectral function and a reduction of the momentum anisotropy of the spectral function. The contrast between the non-perturbative calculations for charge and spin-fluctuations and the comparison with the Eliashberg result is shown in Fig. 5 for $\kappa^2 = 2$. In this case it is clear that the effect of vertex corrections is to make the spectral function sharper than its Eliashberg approximation in the charge-fluctuation case and broader when the quasiparticles are coupled to magnetic fluctuations. For these model parameters, corrections to the Eliashberg approximation reduce the effective charge-mediated interaction and enhance the coupling to magnetic fluctuations.

In Fig. 6 the results of the one-loop calculations in the case of ferromagnetic spin-fluctuation exchange are shown. As could be expected, the spectral function for quasiparticles near the Fermi level does not depend strongly on whether the momentum is near the hot spot, Fig. 6b, or along the diagonal in the Brillouin zone, Fig. 6c, in contrast to the nearly antiferromagnetic case. At the Eliashberg level, the spectral function broadens monotonically as the correlation wavevector κ is reduced and is broader than the corresponding nearly antiferromagnetic case, Fig. 2b,c.

The Monte Carlo results for quasiparticles coupled to ferromagnetic spin-fluctuations are shown in Fig. 7. The tunneling density of states at the Fermi level $N(\omega = 0)$ begins to drop as the parameter $\kappa^2 \leq 0.50$. For $\kappa^2 = 0.25$, the quasiparticle peak has effectively split into two peaks, and a precursor of this effect can be seen at $\kappa^2 = 0.50$. This phenomenon is qualitatively different from what one can obtain at the one-loop level, Fig. 6, just as the pseudogap seen in Fig. 4, when the quasiparticle interactions are mediated by

an antiferromagnetically correlated exchange field. For the larger value of κ^2 where the splitting of the quasiparticle peak is not observed, a comparison of the Monte Carlo results with the one-loop self-consistent calculations shown in Fig. 6 shows that vertex corrections bring about a broadening of the quasiparticle spectral function. Therefore, just as in the antiferromagnetic case, vertex corrections enhance the magnetically-mediated interaction, albeit to a lesser degree, as a close look at Figs. 2,4 and 6,7 indicates. This could explain why qualitative changes from the Eliashberg solution are seen for smaller values of κ^2 for coupling to ferromagnetic than antiferromagnetic fluctuations.

IV. DISCUSSION

For the model considered here, at the one-loop level the exchange of commensurate charge-fluctuations and antiferromagnetic spin-fluctuations yield the same quasiparticle properties. Once vertex corrections are included, the differences between the two cases are evident. In all but one case, $\mathbf{k} = (3\pi/8, 3\pi/8)$ and $\kappa^2 = 4$, corrections to the one-loop approximation make the quasiparticle peak sharper than the Eliashberg result for charge-fluctuations. In the case of antiferromagnetic spin-fluctuations, the quasiparticle peak gets broader as vertex corrections are included and a pseudogap appears for the lower values of κ^2 studied. The difference between the scalar and vector molecular fields appears at the leading vertex correction to the one-loop approximation [14] shown in Fig. 8. The frequency and momentum integrals are the same in both cases since we assume the commensurate charge-fluctuations and antiferromagnetic spin-fluctuations have the same spectrum. However, the spin sums in the two cases are not identical. In the case of a coupling of the molecular field to the quasiparticle spin-density, one gets a factor coming from the Pauli matrices at each vertex in the diagram. For the diagram shown in Fig. 8, this factor is $\sum_{i,j} \sigma^i \sigma^j \sigma^i \sigma^j$. One can split the sum into the $i = j$ and $i \neq j$ terms, and use the fact that $\sigma^i \sigma^i = 1$ and $\sigma^i \sigma^j = -\sigma^j \sigma^i$ if $i \neq j$. Then $\sum_{i,j} \sigma^i \sigma^j \sigma^i \sigma^j = \sum_i \sigma^i \sigma^i \sigma^i \sigma^i - \sum_{i \neq j} \sigma^i \sigma^i \sigma^j \sigma^j = 3 - 6 = -3$. Note that the longitudinal spin-fluctuations contribute a term $\sigma^z \sigma^z \sigma^z \sigma^z = 1$ and thus the

change in sign is caused by the presence of transverse magnetic modes. The corresponding factor in the case of charge-fluctuations is 1, just as in the case without transverse magnetic modes. Coupling the quasiparticles to the spin-density instead of the number density produces a leading vertex correction with the opposite sign. The process depicted in Fig. 8 enhances the magnetic interaction [14] while this same diagram leads to a suppression of the effective interaction in the case of charge-fluctuations. For the range of parameters studied, the Monte Carlo simulations show that this qualitative difference between coupling to magnetic or charge fluctuations persists to all orders, save one case, $\mathbf{k} = (3\pi/8, 3\pi/8)$ and $\kappa^2 = 4$, where vertex corrections enhance the charge-mediated interaction.

As noted above, for large values of κ^2 , vertex corrections do not produce qualitative changes, but merely quantitative ones. One might therefore ask whether one can obtain the non-perturbative results with a one-loop calculation provided the parameters of the theory are renormalized. To illustrate the point, let us focus on the case of antiferromagnetic paramagnons with $\kappa^2 = 2$. One essentially has two parameters one can renormalize, the dimensionless coupling constant $g^2\chi_0/t$ and the inverse correlation length κ . Since vertex corrections make the spectral function broader and the quasiparticle residue smaller, one could attempt to fit the non-perturbative calculations with a one-loop theory with a larger coupling constant $g^2\chi_0/t$ or smaller κ^2 , or a combination of both. If the corrections to the one-loop theory are purely local, it is possible to absorb them in a redefinition of the coupling constant $g^2\chi_0/t$. It turns out that increasing the coupling constant does make the quasiparticle residue smaller but the one-loop spectral function remains too sharp relative to the non-perturbative calculation. By the time $g^2\chi_0/t$ is large enough for the quasiparticle lifetime to be approximately that obtained with the Monte Carlo simulation, the one-loop quasiparticle residue is then too small. One has more success with making κ^2 smaller and Fig. 9 compares the spectral function of the one-loop calculation with $\kappa^2 = 0.25$ with the $A(\mathbf{k}, \omega)$ obtained from the Monte Carlo simulations at $\kappa^2 = 2$. One can get a decent fit near the hot spot at $\mathbf{k} = (\pi, \pi/8)$ but the one-loop spectral function is always more anisotropic in momentum than the non-perturbative $A(\mathbf{k}, \omega)$ for this value of κ^2 .

The most important feature of the calculations presented here is the qualitative change in the quasiparticle spectral function that occurs as the magnetic interaction gets stronger, either on the border of long-range antiferromagnetic or ferromagnetic order. The appearance of a pseudogap in the quasiparticle spectrum near a second-order phase transition as the temperature approaches the critical transition temperature from above was demonstrated for the half-filled Hubbard model [17–19], for a superconducting instability [18,20–23,33,34] and for a Peierls-CDW transition [32]. By contrast, in the model studied in this paper, the quadratic actions of the dynamical molecular fields do not exhibit a phase transition at all (with $\kappa^2 > 0$). It may therefore be somewhat surprising that a pseudogap is observed in the present calculations as the correlation wavevector κ becomes of order one in the nearly antiferromagnetic case and of order one-half for nearly ferromagnetic systems.

The physical origin of the pseudogap was explained in Refs. [17–19] and later in Ref. [32]. Quasiparticles only remain coherent for a finite amount of time. When the distance they can travel during that time becomes shorter than the correlation length of the molecular field, quasiparticles effectively see long-range order. In the presence of long-range antiferromagnetic order, the spin-density-wave quasiparticle spectral function consists of two peaks. In the case of long-range ferromagnetic order the spin-up quasiparticles have an energy shifted downwards, say, relative to the paramagnetic quasiparticle energy while the energy of a spin-down quasiparticle is shifted upwards relative to its energy in the absence of long-range ferromagnetic order. The shifts in energy give rise to corresponding shifts in the quasiparticle peak in the spectral function. Upon averaging over the two spin orientations, the quasiparticle spectral function would then also consist of two peaks, the up-spin and down-spin quasiparticle peaks. In our calculations, when the quasiparticles remain coherent for such a short time that they effectively see long-range order, the spectral functions have characteristics akin to that of the ordered state. For instance, in Fig. 4b, for a coupling of quasiparticles to antiferromagnetic spin-fluctuations, the spectral function $A(\mathbf{k}, \omega)$ for $\kappa^2 = 0.25$ looks like that of a broadened spin-density wave. And in the case of a ferromagnetically correlated molecular field, in Figs. 7b,c, $A(\mathbf{k}, \omega)$ is "spin-split" as κ^2 is reduced, a

feature which can be understood if, during their short lifetime, the quasiparticles effectively see ferromagnetic order, where the moment is equally likely to point up or down, since we are still in the paramagnetic phase.

Quasiparticles only remain coherent for a finite time due to thermal and quantum fluctuations. The question is what is that time scale, or the associated characteristic length scale to be compared against the magnetic correlation length. In the half-filled Hubbard model studied in Refs. [17–19], the renormalized classical regime for the spin-fluctuations always precedes the zero temperature phase transition, and in that regime thermal fluctuations dominate and the relevant characteristic length scale is the thermal quasiparticle de Broglie wavelength $\xi_{th} = v_F/T$ [17–19]. Thermal fluctuations are dominant near the Peierls-CDW transition in two dimensions and the relevant quasiparticle length scale for the onset of the pseudogap also turns out to be ξ_{th} [32]. For the model considered in this paper, however, thermal fluctuations do not appear to dominate. Indeed, the onset of the pseudogap for coupling of quasiparticles to antiferromagnetic fluctuations and the qualitative change seen in the spectral function for coupling to ferromagnetic fluctuations occur for $\xi_{th}\kappa > 1$. The departure from the criterion $\xi_{th}\kappa \approx 1$ for the breakdown of the Midgal approximation is larger in the ferromagnetic case. The above suggests that another, shorter, length scale is relevant in the present case. A possible candidate length scale is the quasiparticle mean-free path.

One can attempt to make this more quantitative by extracting quasiparticle lifetimes and mean-free paths from our numerical results. In order to do this we fit the quasiparticle peak of the spectral function with a Lorentzian $A_L(\mathbf{k}, \omega) = \frac{1}{\pi} \frac{z_{\mathbf{k}}\Gamma_{\mathbf{k}}}{(\omega - E_{\mathbf{k}})^2 + \Gamma_{\mathbf{k}}^2}$ which corresponds to a quasiparticle approximation for the retarded Green's function $\mathcal{G}_R(\mathbf{k}, \omega) = \frac{z_{\mathbf{k}}}{\omega - E_{\mathbf{k}} - i\Gamma_{\mathbf{k}}}$ describing the propagation of quasiparticles of energy $E_{\mathbf{k}}$. $\Gamma_{\mathbf{k}}$ is related to the quasiparticle lifetime $\tau_{\mathbf{k}}$ through $\Gamma_{\mathbf{k}} = \frac{1}{2\tau_{\mathbf{k}}}$. If one ignores the momentum dependence of the self-energy, the quasiparticle residue $z_{\mathbf{k}}$ is related to the ratio of the band to the effective mass $z_{\mathbf{k}} \approx \frac{m}{m^*}$. We define the bare velocity $v_{\mathbf{k}}^{(0)} = \sqrt{(\frac{\partial \epsilon_{\mathbf{k}}}{\partial k_x})^2 + (\frac{\partial \epsilon_{\mathbf{k}}}{\partial k_y})^2}$ where $\epsilon_{\mathbf{k}}$ is the band dispersion relation and the renormalized velocity $v_{\mathbf{k}} = z_{\mathbf{k}}v_{\mathbf{k}}^{(0)}$. The quasiparticle mean-free path is then

approximately $l_{\mathbf{k}} = v_{\mathbf{k}}\tau_{\mathbf{k}}$. The values of $l_{\mathbf{k}}$ one obtains for charge-fluctuations as well as antiferromagnetic and ferromagnetic spin-fluctuations are shown in Fig. 10. In the case of a coupling of quasiparticles to charge-fluctuations, Fig. 10a, $l_{\mathbf{k}} \gg 1/\kappa$ for all the values of κ considered. In this case, the quasiparticles travel far enough during their lifetime to see there is no long-range charge order. In the case of antiferromagnetic spin-fluctuations, Fig. 10b, one sees that at $\mathbf{k} = (\pi, \pi/8)$ $l_{\mathbf{k}} \sim 1/\kappa$ at $\kappa^2 = 1$, and that is where the pseudogap begins to appear in the spectral function, Fig. 4b. At momentum $\mathbf{k} = (3\pi/8, 3\pi/8)$, the mean-free path $l_{\mathbf{k}} > 1/\kappa$ at $\kappa^2 = 1$ and one wouldn't expect a pseudogap. $l_{\mathbf{k}}$ becomes less than the correlation length at the lowest value of κ^2 and one can see hints of a developing pseudogap in the spectral function, Fig. 4c. In the ferromagnetic case, Fig. 10c, the appearance of the two peaks in the spectral function is broadly consistent with the condition $l_{\mathbf{k}} < 1/\kappa$. Note that we are using a simple criterion, in an attempt to capture the essential aspects of the problem, to understand the emergence of a pseudogap in our calculations. The crossover to the new state is likely to depend on other details not taken into account by our criterion and is therefore not expected to occur exactly at $l_{\mathbf{k}} = 1/\kappa$. Moreover, the tails in most of the spectral functions are not Lorentzians and thus our definition of the quasiparticle lifetime is clearly approximate.

We have also extracted mean-free paths for the one-loop approximation using the same methodology (results not shown). For low enough values of κ^2 , one can get in the regime where $l_{\mathbf{k}} \leq 1/\kappa$, but no pseudogap in the spectral function is observed. What is the one-loop approximation missing? A candidate explanation, based on an analogy, is the following. When treating the potential scattering of a particle in a momentum space basis, to lowest order of perturbation theory (Born approximation), one assumes the wavefunction is unchanged, i.e remains a plane-wave. In order to study bound states, in which the wavefunction of the particle is qualitatively different since it is localized, one must treat the scattering events to all orders. By analogy, the Eliashberg approximation does not seem to allow for a change in the quasiparticle wavefunctions which essentially remain plane-waves. In the pseudogap state, the quasiparticle wavefunctions must be qualitatively different and one

must allow the quasiparticles to scatter multiple times against the locally ordered molecular field to produce the required changes in their wavefunctions. It seems one would need to sum an infinite set of spin-fluctuation exchanges.

The "quenched approximation" formulation of the magnetic interaction model actually goes beyond a diagrammatic perturbation expansion. The Green's function, Eq. (2.20), depends on the position, spin, and imaginary time, but also on the parameters of the theory, $\lambda \equiv g^2\chi_0/t$, κ^2 , etc., $\mathcal{G} = \mathcal{G}(i\sigma\tau; j\sigma'\tau'|\lambda, \kappa^2, \dots)$. (To make the dependence on $\lambda = g^2\chi_0/t$ explicit, one simply needs to introduce scaled molecular fields $\mathbf{m} = g\mathbf{M}$. The variance of the new variables is then $g^2\alpha(\mathbf{q}, i\nu_n) \propto g^2\chi(\mathbf{q}, i\nu_n)$). It is clear from Eqs. (2.20,2.4,2.5) that the theory does not make sense for $\lambda < 0$, since the Gaussian distributions of the molecular fields would have a negative variance. This observation means that it is not possible to analytically continue \mathcal{G} to negative values of λ , implying an essential singularity at $\lambda = 0$. The perturbation expansion in powers of $\lambda = 0$ is then an asymptotic rather than convergent series [35]. This opens the possibility for phenomena that lie outside of diagrammatic perturbation theory. Whether the pseudogap state found in the numerical simulations reported on in this paper is precisely one such phenomenon is not presently known to the author.

The results presented here do not imply one couldn't get a pseudogap state when coupling to charge fluctuations. On the basis of the arguments presented above, if one were to increase the strength of the charge correlations or the coupling of quasiparticles to the molecular field Φ , one would get in the regime $l_{\mathbf{k}} \ll 1/\kappa$ and the spectral function ought to resemble that of a broadened charge-density-wave state. Our calculations simply show that one would have to be closer to the ordered state in the case of charge fluctuations than for magnetic fluctuations, under otherwise similar conditions.

V. OUTLOOK

We studied a non-perturbative formulation of the magnetic interaction model, in which quasiparticles are coupled to a Gaussian distributed dynamical molecular exchange field. Far from the magnetic boundary, the type of vertex corrections considered here do not bring about qualitative changes to the quasiparticle spectrum. But as one gets closer to the border of long-range magnetic order, we find, for a range of model parameters, that Migdal's theorem does not apply and the quasiparticle spectrum is qualitatively different from its Eliashberg approximation. The physical origin of the phenomenon is that if the distance quasiparticles can travel during their lifetime becomes shorter than the molecular field correlation length, these quasiparticles effectively see long-range order. When the molecular field correlations are antiferromagnetic, the quasiparticle spectral function has the two-peak structure of a spin-density-wave state, even though there is no spontaneous symmetry breaking. We find that the associated pseudogap is strongly anisotropic in that it vanishes along the diagonal of the Brillouin zone and is large near the zone boundary, in qualitative agreement with photoemission experiments on underdoped cuprates [10]. The anisotropy of the pseudogap found in our calculations simply reflects the anisotropy of the quasiparticle mean-free path. For coupling to ferromagnetic fluctuations, we also find a range of parameters where the quasiparticle spectral function becomes qualitatively different from its one-loop self-consistent approximation. The local ferromagnetic order also leads to a splitting of the quasiparticle peak into two. These pseudogap effects are found to be weaker for nearly ferromagnetic systems than for their nearly antiferromagnetic counterparts, under otherwise similar conditions.

In the standard theory of quantum critical phenomena [28], if $d + z < 4$ where d is the spatial dimensionality and z the dynamical exponent, the mode-mode coupling parameter diverges upon renormalization as one approaches the instability and the critical exponents are different from their mean-field values. Therefore, if $d + z < 4$, one would certainly expect Migdal's theorem to qualitatively break down close enough to the quantum critical

point. However, when $d + z > 4$, the critical exponents take their mean-field values, as in a one-loop calculation. In that case, one could therefore expect, and it is often assumed, that the Eliashberg approximation is at least qualitatively correct. For the magnetic spectrum considered here, Eq. (2.13), $z = 2$ for antiferromagnetic fluctuations and $z = 3$ for ferromagnetic fluctuations. Hence $d + z = 4$, the marginal dimension in the case of antiferromagnetic spin-fluctuations but crucially, $d + z = 5$ in the case of ferromagnetic spin-fluctuations. One could thus have expected that in the latter case, the one-loop self-consistent calculations should be at least qualitatively correct since $d + z > 4$. This is at variance with our results, which show qualitative differences between the non-perturbative calculations and the Eliashberg predictions. Note that the qualitative break down of Migdal's theorem occurs for smaller value of κ^2 in the ferromagnetic case than for antiferromagnetic spin-fluctuations. In that sense the effect of vertex corrections is weaker when $d + z = 5$ compared to the case $d + z = 4$, which is what is expected.

To summarize, an often assumed criterion for the qualitative applicability of the Eliashberg theory near an instability, namely $d + z > 4$, is clearly a necessary condition but the calculations presented here show that it is not a sufficient one. This result may point to certain limitations of the standard theory of quantum critical phenomena [28], which has recently been criticized by Anderson [36].

The crucial role of dimensionality for pseudogap phenomena has been emphasized by Tremblay and collaborators [17,18,21] and by Preosti et al. [37]. Since critical fluctuations responsible for the precursor pseudogap are much stronger in two dimensions than for three dimensional systems, they find that pseudogap phenomena are much weaker in three dimensions. One would expect similar results for the magnetic interaction model studied in the present paper. The role of lattice anisotropy is already important at the Eliashberg level [3–6], because of the increased phase space of soft magnetic fluctuations in lower dimensional systems. This phase space argument leads one to expect weaker vertex corrections to the Eliashberg theory of the magnetic interaction model, and hence weaker pseudogap effects in isotropic three dimensional systems.

The results presented here raise a number of obvious questions, which we hope to answer in the future. For instance, what are the corrections to the Eliashberg theory for the superconducting transition temperature to the $d_{x^2-y^2}$ pairing state? We have studied corrections to quasiparticle spectral properties, and found that vertex corrections can produce a pseudogap in the quasiparticle spectrum. When the magnetic correlations are weak enough vertex corrections do not bring about qualitative changes but nevertheless reduce the quasiparticle lifetime. The above effects are expected to suppress magnetic pairing. But one must also include in the calculation of the superconducting transition temperature the corresponding corrections to the pairing interaction. In leading order, it was shown [14] that vertex corrections lead to a stronger pairing interaction in the d-wave channel. There may therefore be some cancellation of errors, at least in some range of model parameters. At this stage, however, one can only speculate about the effect of vertex corrections on the Eliashberg theory of the superconducting transition temperature.

Transport and thermodynamic properties in the quenched approximation would also be of great interest. The calculations in Ref. [32] showed that the pseudogap in the single particle density of states also appeared in the two-particle Green's functions such as the optical conductivity and the uniform Pauli susceptibility. I therefore expect that the pseudogap observed in the quasiparticle spectral function will show up in the thermodynamic and transport properties of the model studied here. The extent to which the model is able to explain the normal state experimental data on the underdoped cuprates is an open question.

Our simplifying assumptions, which were born out of the necessity to carry out the calculations in a reasonable amount of time, should be relaxed. The dynamical molecular field correlation function which enters their distribution was taken to be of the same functional form for all the calculations. In Nature, however, the distribution function of the molecular field experienced by one quasiparticle is determined self-consistently by all of the other quasiparticles in the system. It is therefore expected to change as the nature of the quasiparticle spectrum changes. One should also study the effect of mode-mode coupling terms which were ignored in the present study. Monien has recently carried out such a study for

a model of the one-dimensional Peierls-CDW [38].

There is no doubt that the extension of the theory to deal with effects ignored here will bring about quantitative changes to our results. It will be of great interest to figure out if and for what model parameters our results are modified qualitatively. I would like to think that the physical origin of the emergence of a pseudogap in the quasiparticle spectrum will turn out to be independent of the details of the model.

VI. ACKNOWLEDGMENTS

I would like to thank P. Coleman, J.R. Cooper, P.B. Littlewood, G.G. Lonzarich, J. Loram, and D. Pines for discussions on this and related topics. We acknowledge the support of the EPSRC, the Newton Trust and the Royal Society.

VII. APPENDIX: GREEN'S FUNCTIONS

In this appendix we derive the mathematical formulas for the single-particle Green's functions in a fluctuating exchange or scalar field. We also give the algorithm for the numerically stable and efficient calculation of such Green's functions. We shall make use of fermion coherent states and will derive the path-integral for an anti-normal ordered [39] Hamiltonian quadratic in the fermion field operators.

We first need an identity for expressing the exponential of the quadratic form

$$\hat{Q}_A = \sum_{i,j} \psi_i A_{i,j} \psi_j^\dagger \quad (7.1)$$

in terms of fermion coherent states. In the above expression, $A = A^\dagger$ is a Hermitian matrix of dimension N and $\{\psi\}, \{\psi^\dagger\}$ are fermion operators. One has:

$$\exp \left(\sum_{i,j} \psi_i A_{i,j} \psi_j^\dagger \right) = \int \left[\prod_{i=1}^N d\xi_i^* d\xi_i \right] |\xi\rangle \exp \left(\sum_{i,j} \xi_i (e^A)_{i,j} \xi_j^* \right) \langle \xi| \quad (7.2)$$

where $\{\xi^*\}, \{\xi\}$ are Grassmann numbers. This identity is proved by going into a basis in which the matrix A is diagonal. Let U be the unitary transformation that diagonalizes A

$$U^\dagger A U = \Lambda \equiv \text{diag}(\lambda_1, \dots, \lambda_N) \quad (7.3)$$

In terms of the new fermion fields $\{\Phi\}, \{\Phi^\dagger\}$

$$\psi_i = \sum_j U_{i,j}^* \Phi_j \quad (7.4)$$

$$\psi_i^\dagger = \sum_j U_{i,j} \Phi_j^\dagger \quad (7.5)$$

$$\Phi_i = \sum_j U_{j,i} \psi_j \quad (7.6)$$

$$\Phi_i^\dagger = \sum_j U_{j,i}^* \psi_j^\dagger \quad (7.7)$$

the quadratic form Eq. (7.1) becomes $\hat{Q}_A = \sum_i \lambda_i \Phi_i \Phi_i^\dagger$. Since $(\Phi_i \Phi_i^\dagger)^n = \Phi_i \Phi_i^\dagger$ for $n = 1, 2, \dots, \infty$, and the terms with different indices i commute with one another, one has

$$\exp(\hat{Q}_A) = \prod_i \exp(\lambda_i \Phi_i \Phi_i^\dagger) = \prod_i \left\{ 1 + [\exp(\lambda_i) - 1] \Phi_i \Phi_i^\dagger \right\} \quad (7.8)$$

Expanding the product into sums yields

$$\begin{aligned} \exp(\hat{Q}_A) &= 1 + \sum_{i_1} [\exp(\lambda_{i_1}) - 1] \Phi_{i_1} \Phi_{i_1}^\dagger + \sum_{i_1 < i_2} [\exp(\lambda_{i_1}) - 1] [\exp(\lambda_{i_2}) - 1] \Phi_{i_1} \Phi_{i_1}^\dagger \Phi_{i_2} \Phi_{i_2}^\dagger \\ &+ \sum_{i_1 < i_2 < i_3} [\exp(\lambda_{i_1}) - 1] [\exp(\lambda_{i_2}) - 1] [\exp(\lambda_{i_3}) - 1] \Phi_{i_1} \Phi_{i_1}^\dagger \Phi_{i_2} \Phi_{i_2}^\dagger \Phi_{i_3} \Phi_{i_3}^\dagger + \dots \\ &+ \sum_{i_1 < \dots < i_N} [\exp(\lambda_{i_1}) - 1] \dots [\exp(\lambda_{i_N}) - 1] \Phi_{i_1} \Phi_{i_1}^\dagger \dots \Phi_{i_N} \Phi_{i_N}^\dagger \end{aligned} \quad (7.9)$$

Since in the various sums one has $i_1 \neq i_2 \neq i_3 \dots \neq i_N$, one can straightforwardly anti-normal order the terms

$$\Phi_{i_1} \Phi_{i_1}^\dagger \Phi_{i_2} \Phi_{i_2}^\dagger = \Phi_{i_2} \Phi_{i_1} \Phi_{i_1}^\dagger \Phi_{i_2}^\dagger \quad (7.10)$$

$$\Phi_{i_1} \Phi_{i_1}^\dagger \Phi_{i_2} \Phi_{i_2}^\dagger \Phi_{i_3} \Phi_{i_3}^\dagger = \Phi_{i_3} \Phi_{i_2} \Phi_{i_1} \Phi_{i_1}^\dagger \Phi_{i_2}^\dagger \Phi_{i_3}^\dagger \quad (7.11)$$

$$\Phi_{i_1} \Phi_{i_1}^\dagger \Phi_{i_2} \Phi_{i_2}^\dagger \dots \Phi_{i_N} \Phi_{i_N}^\dagger = \Phi_{i_N} \Phi_{i_{N-1}} \dots \Phi_{i_1} \Phi_{i_1}^\dagger \Phi_{i_2}^\dagger \dots \Phi_{i_N}^\dagger \quad (7.12)$$

We can now insert a resolution of the identity between the annihilation and creation operators. For instance

$$\Phi_{i_3} \Phi_{i_2} \Phi_{i_1} \Phi_{i_1}^\dagger \Phi_{i_2}^\dagger \Phi_{i_3}^\dagger = \Phi_{i_3} \Phi_{i_2} \Phi_{i_1} \int \left[\prod_{i=1}^N d\xi_i^* d\xi_i \right] |\xi\rangle \exp\left(-\sum_i \xi_i^* \xi_i\right) \langle \xi | \Phi_{i_1}^\dagger \Phi_{i_2}^\dagger \Phi_{i_3}^\dagger$$

$$\begin{aligned}
&= \int \prod_{i=1}^N d\xi_i^* d\xi_i \xi_{i_3} \xi_{i_2} \xi_{i_1} |\xi\rangle \exp\left(-\sum_i \xi_i^* \xi_i\right) \langle \xi | \xi_{i_1}^* \xi_{i_2}^* \xi_{i_3}^* \\
&= \int \left[\prod_{i=1}^N d\xi_i^* d\xi_i\right] \xi_{i_1} \xi_{i_1}^* \xi_{i_2} \xi_{i_2}^* \xi_{i_3} \xi_{i_3}^* \exp\left(-\sum_i \xi_i^* \xi_i\right) |\xi\rangle \langle \xi|
\end{aligned}$$

Applying the above operation to every term in the sum in Eq. (7.9) one obtains

$$\begin{aligned}
\exp(\hat{Q}_A) &= \int \left[\prod_{i=1}^N d\xi_i^* d\xi_i\right] |\xi\rangle \exp\left(-\sum_i \xi_i^* \xi_i\right) \prod_{i=1}^N [1 + (e^{\lambda_i} - 1) \xi_i \xi_i^*] \langle \xi| \\
&= \int \left[\prod_{i=1}^N d\xi_i^* d\xi_i\right] |\xi\rangle \exp\left(-\sum_i \xi_i^* \xi_i\right) \exp\left(\sum_i (e^{\lambda_i} - 1) \xi_i \xi_i^*\right) \langle \xi| \\
&= \int \left[\prod_{i=1}^N d\xi_i^* d\xi_i\right] |\xi\rangle \exp\left(\sum_i e^{\lambda_i} \xi_i \xi_i^*\right) \langle \xi|
\end{aligned} \tag{7.13}$$

Going back to the original representation in which the matrix A is not diagonal yields Eq. (7.2). If we have another quadratic form

$$\hat{Q}_B = \sum_{ij} \psi_i B_{i,j} \psi_j^\dagger \tag{7.14}$$

where $B = B^\dagger$ is a Hermitian matrix of dimension N , it is a simple exercise in Grassmann integration to show that

$$\exp(\hat{Q}_A) \exp(\hat{Q}_B) = \int \left[\prod_{i=1}^N d\xi_i^* d\xi_i\right] |\xi\rangle \exp\left(\sum_{ij} \xi_i (e^A e^B)_{i,j} \xi_j^*\right) \langle \xi| \tag{7.15}$$

To prove the above identity one uses the coherent state representation Eq. (7.2) for $\exp(\hat{Q}_A)$ and $\exp(\hat{Q}_B)$

$$\exp(\hat{Q}_A) = \int \left[\prod_{i=1}^N d\xi_i^* d\xi_i\right] |\xi\rangle \exp\left(\sum_{ij} \xi_i (e^A)_{i,j} \xi_j^*\right) \langle \xi| \tag{7.16}$$

$$\exp(\hat{Q}_B) = \int \left[\prod_{i=1}^N d\eta_i^* d\eta_i\right] |\eta\rangle \exp\left(\sum_{ij} \eta_i (e^B)_{i,j} \eta_j^*\right) \langle \eta| \tag{7.17}$$

Integrating over the Grassmann variables $\{\xi_i^*\}$ and $\{\eta_i\}$ yields Eq. (7.15).

The imaginary time single-particle Green's function in a time dependent field is given by the usual expression

$$\begin{aligned}
G(i\sigma\tau; j\sigma'\tau') &= -\langle T_\tau \{ \psi_{i\sigma}(\tau) \psi_{j\sigma'}^\dagger(\tau') \} \rangle \\
&= -\frac{1}{\mathcal{Z}} \text{Tr} \left[T_\tau \left\{ \exp\left(-\int_0^\beta \hat{h}(s) ds\right) \psi_{i\sigma}(\tau) \psi_{j\sigma'}^\dagger(\tau') \right\} \right]
\end{aligned} \tag{7.18}$$

$$\mathcal{Z} = \text{Tr} \left[T_\tau \exp\left(-\int_0^\beta \hat{h}(s) ds\right) \right] \tag{7.19}$$

where the time dependent Hamiltonian $\hat{h}(\tau)$ is given by Eq. (2.2) and Eq. (2.3) for coupling to a fluctuating exchange or scalar field respectively. The trace is over the fermion fields. For ease of notation, we have dropped the explicit dependence of $G(i\sigma\tau; j\sigma'\tau')$ on the molecular field. Because of the time ordering operator, one must distinguish the two cases $\tau > \tau'$ and $\tau \leq \tau'$.

$$G(i\sigma\tau; j\sigma'\tau') = -\frac{1}{\mathcal{Z}} \text{Tr} \left[\left\{ T_\tau \exp \left(- \int_\tau^\beta \hat{h}(s) ds \right) \right\} \psi_{i\sigma}(\tau) \left\{ T_{\tau'} \exp \left(- \int_{\tau'}^\tau \hat{h}(s) ds \right) \right\} \psi_{j\sigma'}^\dagger(\tau') \right. \\ \left. \times \left\{ T_\tau \exp \left(- \int_0^\tau \hat{h}(s) ds \right) \right\} \right] \quad \tau > \tau' \quad (7.20)$$

$$G(i\sigma\tau; j\sigma'\tau') = -\frac{1}{\mathcal{Z}} \text{Tr} \left[\left\{ T_\tau \exp \left(- \int_\tau^\beta \hat{h}(s) ds \right) \right\} \psi_{j\sigma'}^\dagger(\tau') \left\{ T_{\tau'} \exp \left(- \int_{\tau'}^\tau \hat{h}(s) ds \right) \right\} \psi_{i\sigma}(\tau) \right. \\ \left. \times \left\{ T_{\tau'} \exp \left(- \int_0^{\tau'} \hat{h}(s) ds \right) \right\} \right] \quad \tau \leq \tau' \quad (7.21)$$

The imaginary times τ and τ' are discretized such that $\tau = \Delta\tau m$ $m = 0, 1, \dots, L_t$, $\tau' = \Delta\tau m'$ $m' = 0, 1, \dots, L_t$, where $\Delta\tau = \frac{\beta}{L_t}$. One then uses the Trotter break-up for the Hamiltonian in an exchange, Eq. (2.2), or scalar field, Eq. (2.3), and hence $\exp(-\Delta\tau \hat{h}(m\Delta\tau)) \approx \exp(-\Delta\tau \hat{h}_1(m\Delta\tau)) \exp(-\Delta\tau \hat{h}_0(m\Delta\tau))$. Up to an unimportant constant, the anti-normal ordered hopping Hamiltonian \hat{h}_0 , Eq. (2.1) is written as

$$\hat{h}_0 = \sum_{i,\sigma;j\sigma'} \psi_{i\sigma} T_{i\sigma,j\sigma'} \psi_{j\sigma'}^\dagger \quad (7.22)$$

$$T_{i\sigma,j\sigma'} = (t_{ij} + \mu \delta_{i,j}) \delta_{\sigma,\sigma'} \quad (7.23)$$

Similarly, up to constant terms that drop out of the expression for the single particle Green's function, the Hamiltonian for the coupling to the fluctuating field is written as

$$\hat{h}_1(m\Delta\tau) = \sum_{i\sigma;j\sigma'} \psi_{i\sigma} A_{i\sigma,j\sigma'}(m) \psi_{j\sigma'}^\dagger \quad (7.24)$$

$$A_{i\sigma,j\sigma'}(m) = \frac{g}{\sqrt{3}} \delta_{i,j} \left[M_i^z(m\Delta\tau) \delta_{\sigma,\uparrow} \delta_{\sigma',\uparrow} - M_i^z(m\Delta\tau) \delta_{\sigma,\downarrow} \delta_{\sigma',\downarrow} \right. \\ \left. + (M_i^x(m\Delta\tau) + iM_i^y(m\Delta\tau)) \delta_{\sigma,\uparrow} \delta_{\sigma',\downarrow} + (M_i^x(m\Delta\tau) - iM_i^y(m\Delta\tau)) \delta_{\sigma,\downarrow} \delta_{\sigma',\uparrow} \right] \quad (7.25)$$

$$A_{i\sigma,j\sigma'}(m) = g \delta_{i,j} \delta_{\sigma,\sigma'} \Phi_i(m\Delta\tau) \quad (7.26)$$

where Eq. (7.25) and Eq. (7.26) are for a fluctuating exchange and scalar field respectively. Making use of Eqs. (7.2,7.15), one has

$$\begin{aligned}\exp(-\Delta\tau\hat{h}(m\Delta\tau)) &\approx \exp(-\Delta\tau\hat{h}_1(m\Delta\tau))\exp(-\Delta\tau\hat{h}_0(m\Delta\tau)) \\ &= \int d\mu(\xi)|\xi\rangle \exp\left(\sum_{i\sigma,j\sigma'} \xi_{i\sigma}[B_m]_{i\sigma,j\sigma'}\xi_{j\sigma'}^*\right) \langle\xi| \end{aligned} \quad (7.27)$$

$$B_m = \exp(-\Delta\tau A(m))\exp(-\Delta\tau T) \quad (7.28)$$

where from now on we use $d\mu(\xi)$ to denote the Grassmann integration measure

$$d\mu(\xi) \equiv [\prod_{i\sigma} d\xi_{i\sigma}^* d\xi_{i\sigma}] \quad (7.29)$$

In the case of coupling to a scalar field

$$[\exp(-\Delta\tau A(m))]_{i\sigma,j\sigma'} = \delta_{i,j}\delta_{\sigma\sigma'} \exp(-g\Delta\tau\Phi_i(m\Delta\tau)) \quad (7.30)$$

The case of the exchange field is slightly more complicated:

$$[\exp(-\Delta\tau A(m))]_{i\sigma,j\sigma'} = \delta_{i,j}[\exp(-\Delta\tau a_i(m))]_{\sigma,\sigma'} \quad (7.31)$$

$$\exp(-\Delta\tau a_i(m)) = \begin{pmatrix} c - s\mathcal{M}_i^z(m\Delta\tau) & -s\mathcal{M}_i^+(m\Delta\tau) \\ -s\mathcal{M}_i^-(m\Delta\tau) & c + s\mathcal{M}_i^z(m\Delta\tau) \end{pmatrix} \quad (7.32)$$

$$c = \cosh(g\Delta\tau|\mathbf{M}_i(m\Delta\tau)|/\sqrt{3}) \quad (7.33)$$

$$s = \sinh(g\Delta\tau|\mathbf{M}_i(m\Delta\tau)|/\sqrt{3}) \quad (7.34)$$

$$\mathcal{M}_i^z(m\Delta\tau) = \frac{M_i^z(m\Delta\tau)}{|\mathbf{M}_i(m\Delta\tau)|} \quad (7.35)$$

$$\mathcal{M}_i^\pm(m\Delta\tau) = \frac{M_i^x(m\Delta\tau) \pm iM_i^y(m\Delta\tau)}{|\mathbf{M}_i(m\Delta\tau)|} \quad (7.36)$$

$$|\mathbf{M}_i(m\Delta\tau)| = \sqrt{[M_i^x(m\Delta\tau)]^2 + [M_i^y(m\Delta\tau)]^2 + [M_i^z(m\Delta\tau)]^2} \quad (7.37)$$

Matrix multiplication by $\exp(-\Delta\tau A(m))$ is most easily done in real space. We have implemented the matrix multiplication by $\exp(-\Delta\tau T)$ by means of the Fast Fourier transform instead of the usual checkerboard decomposition. In the discretized imaginary time version,

$$\begin{aligned}T_\tau \exp\left(-\int_0^\beta \hat{h}(s)ds\right) &\approx \exp(-\Delta\tau\hat{h}(\Delta\tau L_t)) \dots \exp(-\Delta\tau\hat{h}(\Delta\tau)) \\ &= \int d\mu(\xi)|\xi\rangle \exp\left(\sum_{i\sigma,j\sigma'} \xi_{i\sigma}[B_{L_t}B_{L_t-1}\dots B_1]_{i\sigma,j\sigma'}\xi_{j\sigma'}^*\right) \langle\xi| \end{aligned} \quad (7.38)$$

Note that we choose to approximate the imaginary time integral of a function in an interval of length $\Delta\tau$ by $\Delta\tau$ times the value of the function at the upper limit of the

interval. The calculation of the normalization factor \mathcal{Z} , Eq. (7.19), then becomes a simple exercise in Grassmann integration

$$\begin{aligned}\mathcal{Z} &= \int d\mu(\eta)d\mu(\xi) \langle -\eta|\xi \rangle \exp\left(-\sum_{i\sigma}\eta_{i\sigma}^*\eta_{i\sigma} + \sum_{i\sigma j\sigma'}\xi_{i\sigma}[B_{L_t}B_{L_t-1}\dots B_1]_{i\sigma,j\sigma'}\xi_{j\sigma'}^*\right) \langle \xi|\eta \rangle \\ &= \text{Det}[1 + B_1^T B_2^T \dots B_{L_t}^T] = \text{Det}[1 + B_0^T B_1^T \dots B_{L_t-1}^T]\end{aligned}\quad (7.39)$$

where B_m^T is the transpose of the matrix B_m and in the last line we have used the periodicity of the exchange and scalar fields which implies $B_{L_t} = B_0$ and multiplied the expression by $1 = \text{Det}[B_0^T B_0^{T-1}]$.

The remainder of the calculation of the Green's function proceeds along similar lines. Consider the case $m > m'$. One has

$$\begin{aligned}T_\tau \exp\left(-\int_\tau^\beta \hat{h}(s)ds\right) &\approx \exp(-\Delta\tau \hat{h}(\Delta\tau L_t)) \dots \exp(-\Delta\tau \hat{h}(\Delta\tau(m+1))) \\ &= \int d\mu(\xi)|\xi \rangle \exp\left(\sum_{i\sigma j\sigma'}\xi_{i\sigma}[B_{L_t}B_{L_t-1}\dots B_{m+1}]_{i\sigma,j\sigma'}\xi_{j\sigma'}^*\right) \langle \xi|\end{aligned}\quad (7.40)$$

with similar expressions for $T_\tau \exp\left(-\int_{\tau'}^\tau \hat{h}(s)ds\right)$ and $T_\tau \exp\left(-\int_0^{\tau'} \hat{h}(s)ds\right)$. After straightforward algebraic manipulations, one arrives at:

$$\begin{aligned}G(i\sigma m, j\sigma' m') &= -\frac{1}{\mathcal{Z}} \int d\mu(\xi)d\mu(\eta)d\mu(\rho)d\mu(\phi) \exp\left(-\sum_{i\sigma}\xi_{i\sigma}^*\xi_{i\sigma}\right) \exp\left(-\sum_{i\sigma}\xi_{i\sigma}^*\eta_{i\sigma}\right) \\ &\quad \exp\left(\sum_{i\sigma}\eta_{i\sigma}^*\rho_{i\sigma}\right) \exp\left(\sum_{i\sigma}\rho_{i\sigma}^*\phi_{i\sigma}\right) \rho_{i\sigma}\rho_{j\sigma'}^* \exp\left(-\sum_{i\sigma,j,\sigma'}\eta_{i\sigma}M_{i\sigma,j\sigma'}^\eta\eta_{j\sigma'}^*\right) \\ &\quad \exp\left(-\sum_{i\sigma j\sigma'}\rho_{i\sigma}M_{i\sigma,j\sigma'}^\rho\rho_{j\sigma'}^*\right) \exp\left(-\sum_{i\sigma j\sigma'}\phi_{i\sigma}M_{i\sigma,j\sigma'}^\phi\phi_{j\sigma'}^*\right)\end{aligned}\quad (7.41)$$

$$M^\eta = B_{L_t}B_{L_t-1}\dots B_{m+1}\quad (7.42)$$

$$M^\rho = B_m B_{m-1} \dots B_{m'+1}\quad (7.43)$$

$$M^\phi = B_{m'} B_{m'-1} \dots B_1\quad (7.44)$$

The integral over the quadratic form is easily computed. The calculation in the case $m \leq m'$ proceeds along similar lines and we just quote the final answer. The single particle Green's function is given by the following matrix expressions

$$G(m, m') = \begin{cases} -B_{m+1}^T \dots B_{L_t}^T B_1^T \dots B_{m'}^T [1 + B_{m'+1}^T \dots B_{L_t}^T B_1^T \dots B_{m'}^T]^{-1} & \text{if } m > m' \\ B_{m+1}^T B_{m+2}^T \dots B_{m'}^T [1 + B_{m'+1}^T \dots B_{L_t}^T B_1^T \dots B_{m'}^T]^{-1} & \text{if } m \leq m' \end{cases}\quad (7.45)$$

Note that these expressions differ from those of Ref. [40] since these authors are using the standard formulation of the path integral with normal ordered operators, instead of the anti-normal ordering used here. The numerical calculation of the single particle Green's function, Eq. (7.45), is complicated by the fact that the matrix products entering the above expressions are seriously ill-conditioned [41]. I have found that the Gram-Schmidt matrix factorization algorithm of Ref. [41] can be unstable at sufficiently low temperatures and for strongly fluctuating molecular fields. I therefore use an alternative way to compute the Green's function which I have found to be particularly stable. It is based on the matrix identities:

$$(1 + A_1 A_2)^{-1} = T_2 [1 - T_1 - T_2 + 2T_1 T_2]^{-1} T_1 \quad (7.46)$$

$$A_2 (1 + A_1 A_2)^{-1} = [1 - T_2] [1 - T_1 - T_2 + 2T_1 T_2]^{-1} T_1 \quad (7.47)$$

$$T_i = (1 + A_i)^{-1} \quad (7.48)$$

In practice we calculate $G(m, 0)$ and $G(0, m')$. The above matrix identities can be used recursively to calculate these Green's functions in a stable manner. The matrices A_1, A_2 are taken as products of B^T matrices. The number of B^T matrices in a "block" is chosen to be the maximum number such that $(1 + A_1), (1 + A_2)$ can be inverted without significant loss of precision. One can then obtain the Green's functions $G(m, 0)$ and $G(0, m')$ at a subset of values m, m' . The Green's function for the other values of m, m' can be obtained by propagating forward or backward in time. For example, $G(m + 1, 0) = [B_{m+1}^T]^{-1} G(m, 0)$. We leave it to the reader to fill in the details.

REFERENCES

- [1] N.E. Bickers, D.J. Scalapino and S.R. White, Phys. Rev. Lett. **62**, 961 (1989). T.Moriya, Y. Takahashi and K. Ueda, J. Phys. Soc. Jpn. **52**, 2905 (1990). P. Monthoux, A.V. Balatsky and D. Pines, Phys. Rev. Lett. **67**, 3448 (1991).
- [2] E.R. Dobbs, "Helium Three", Oxford University Press (2001).
- [3] S. Nakamura, T. Moriya and K. Ueda, J. Phys. Soc. Jpn. **65**, 4026 (1996).
- [4] R. Arita, K. Kuroki, and H. Aoki, Phys. Rev. B **60**, 14585 (1999) ; J. Phys. Soc. Jpn. **69**, 1181 (2000).
- [5] P. Monthoux and G.G. Lonzarich, Phys. Rev. B **63**, 054529 (2001).
- [6] P. Monthoux and G.G. Lonzarich, Phys. Rev. B **66**, 224504 (2002).
- [7] C. Petrovic, P.G. Pagliuso, M.F. Hundley, R. Movshovich, J.L. Sarrao, J.D. Thompson, Z. Fisk and P. Monthoux, J. Phys. C **13**, L337 (2001).
- [8] P. Monthoux and G.G. Lonzarich, Phys. Rev. B **59**, 14598 (1999).
- [9] S.S. Saxena, P. Argawal, K. Ahilan, F.M. Grosche, R.K.W. Haselwimmer, M.J. Steiner, E. Pugh, I.R. Walker, S.R. Julian, P. Monthoux, G.G. Lonzarich, A. Huxley, I. Sheikin, D. Braithwaite, J. Flouquet, Nature **406**, 587 (2000).
- [10] H. Ding, T. Yokoya, J.C. Campuzano, T. Takahashi, M. Randeria, M.R. Norman, T. Mochiku, K. Kadowaki, J. Giapintzakis, Nature **382**, 51 (1996). A.G. Loeser, Z.X. Shen, D.S. Dessau, D.S. Marshall, C.H. Park, P. Fournier, A. Kapitulnik, Science, **273**, 325 (1996).
- [11] J.W. Loram, J. Luo, J.R. Cooper, W.Y. Liang, J.L. Tallon, J. Phys. Chem. Solids **62**, 59 (2001). J.W. Loram, K.A. Mirza, J.R. Cooper, J.L. Talloon, J. Phys. Chem. Solids **59**, 2091 (1998).
- [12] V.A. Sidorov, M. Nicklas, P.G. Pagliuso, J.L. Sarrao, Y. Bang, A.V. Balatsky, J.D.

- Thompson Phys. Rev. Lett. **89**, 157004 (2002).
- [13] J.R. Schrieffer, J. Low Temp. Phys. **99**, 397 (1995).
- [14] P. Monthoux, Phys. Rev. B **55**, 15261 (1997). A.V. Chubukov, P. Monthoux and D.R. Morr, Phys. Rev. B **56**, 7789 (1997).
- [15] D.J. Scalapino, in "Superconductivity", edited by R.D. Parks, Marcel Dekker, New York, (1969).
- [16] N.E. Bickers and D.J. Scalapino, Ann. Phys. (N.Y.) **193**, 206 (1989).
- [17] Y.M. Vilk and A.-M. S. Tremblay, Europhysics Lett. **33**, 159 (1996).
- [18] Y.M. Vilk and A.-M. S. Tremblay, J. Phys. I, France **7**, 1309 (1997).
- [19] S. Moukouri, S. Allen, F. Lemay, B. Kyung, D. Poulin. Y. M. Vilk and A.-M. S. Tremblay, Phys. Rev. B **61**, 7887 (2000).
- [20] Y.M. Vilk, S. Allen, H. Touchette, S. Moukouri, L. Chen and A.-M. S. Tremblay, J. Phys. Chem. Solids, **59**, 1873 (1998).
- [21] S. Allen, H. Touchette, S. Moukouri, Y.M. Vilk, and A.-M. S. Tremblay, Phys. Rev. Lett. **83**, 4128 (1999).
- [22] S. Allen and A.-M. S. Tremblay, Phys. Rev. B **64**, 075115 (2001).
- [23] B. Kyung, S. Allen, and A.-M. S. Tremblay, Phys. Rev. B **64**, 075116 (2001).
- [24] S. Fujimoto, J. Phys. Soc. Jpn **71**, 1230 (2002).
- [25] P. Monthoux, Phil. Mag. B **79**, 15 (1999).
- [26] E. Marinari, G. Parisi and C. Rebbi, Nucl. Phys. **B** 190, 734 (1981).
- [27] A. Posazhennikova and P. Coleman, cond-mat/0209014.
- [28] J.A. Hertz, Phys. Rev. B **14**, 1165 (1976). A.J. Millis, Phys. Rev. B **48**, 7183 (1993).

- [29] J. Schmalian, D. Pines and B.P. Stojkovic, Phys. Rev. B **60**, 667 (1999).
- [30] H.J. Vidberg and J.W. Serene, J. Low Temp. Phys. **29**, 179 (1977).
- [31] M. Jarrell and J.E. Gubernatis, Phys Rep **269**, 134 (1996).
- [32] P. Monthoux and D.J. Scalapino, Phys. Rev. B **65**, 235104 (2002).
- [33] D. Rohe and W. Metzner, Phys. Rev. B **63**, 224509 (2001).
- [34] T. Eckl, D.J. Scalapino, E. Arrigoni, W. Hanke Phys. Rev. B **66**, 140510 (2002).
- [35] J.W. Negele and H. Orland, *Quantum Many-Particle Systems*, Addison-Wesley (1988).
See chapter 7 for such an example.
- [36] P.W. Anderson, Physica B **318**, 28 (2002).
- [37] G. Preosti, Y.M. Vilk, M.R. Norman, Phys. Rev. B **59**, 1474 (1999).
- [38] H. Monien, Phys. Rev. Lett **87**, 126402 (2001).
- [39] I learned this formulation of functional integrals from Patrick Lee.
- [40] R. Blankenbecler, D.J. Scalapino and R.L. Sugar, Phys. Rev. D **24**, 2278 (1981).
- [41] S.R. White, D.J. Scalapino, R.L. Sugar, E.Y. Loh, J.E. Gubernatis, R.T. Scalettar,
Phys. Rev. B **40**, 506 (1989).

FIGURES

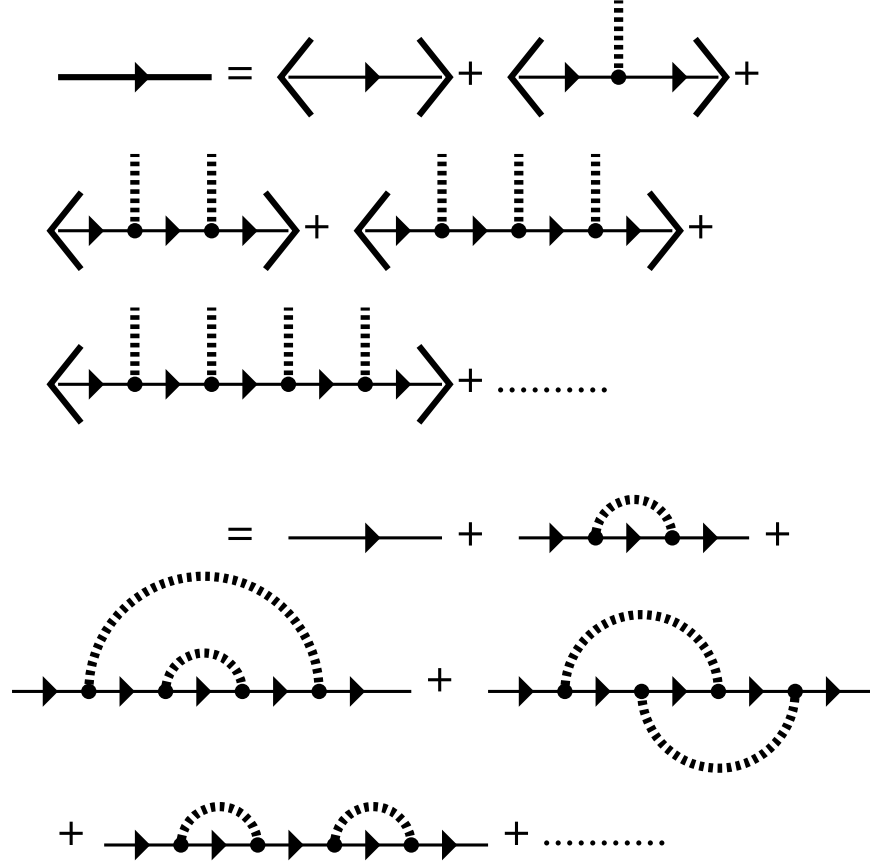
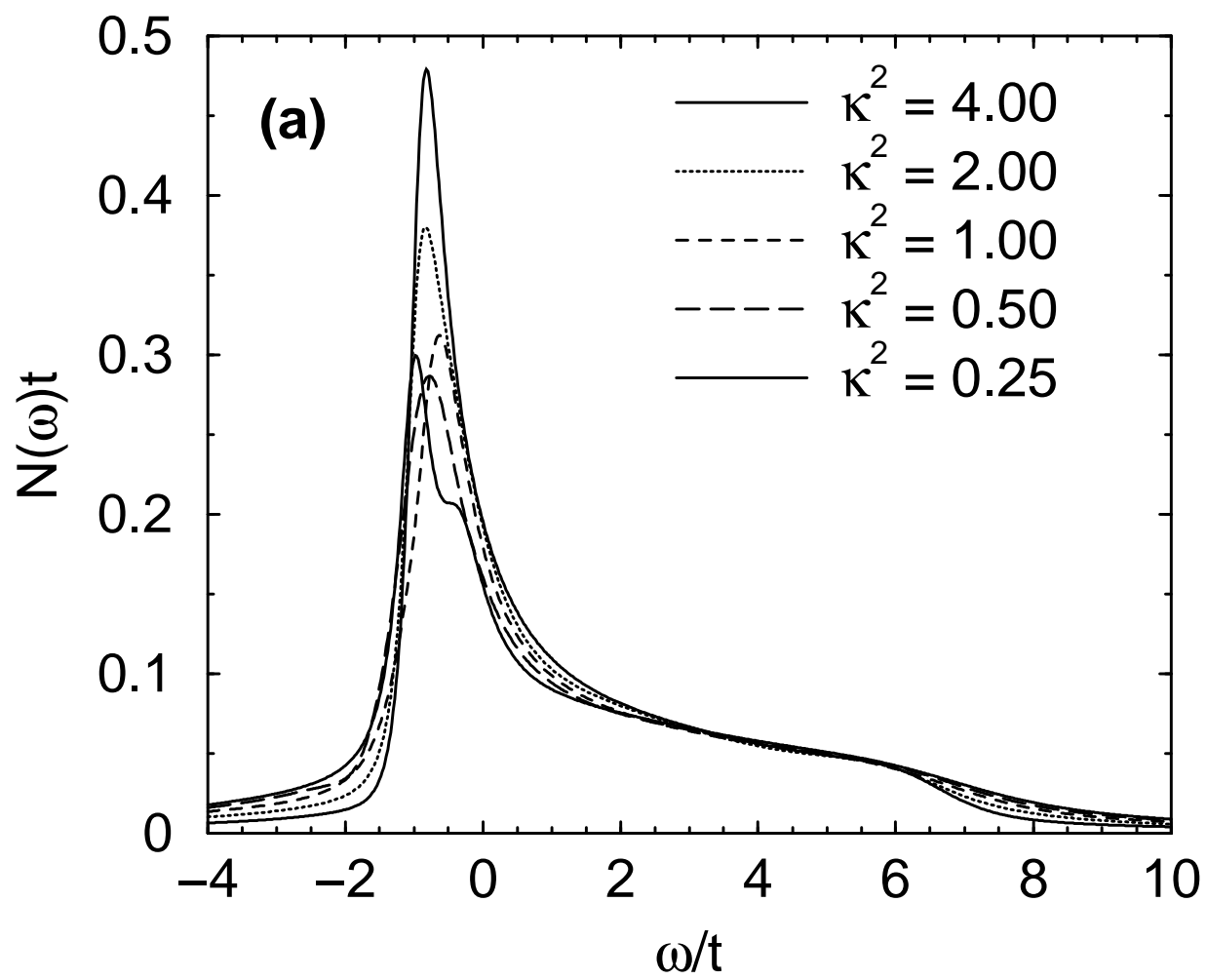
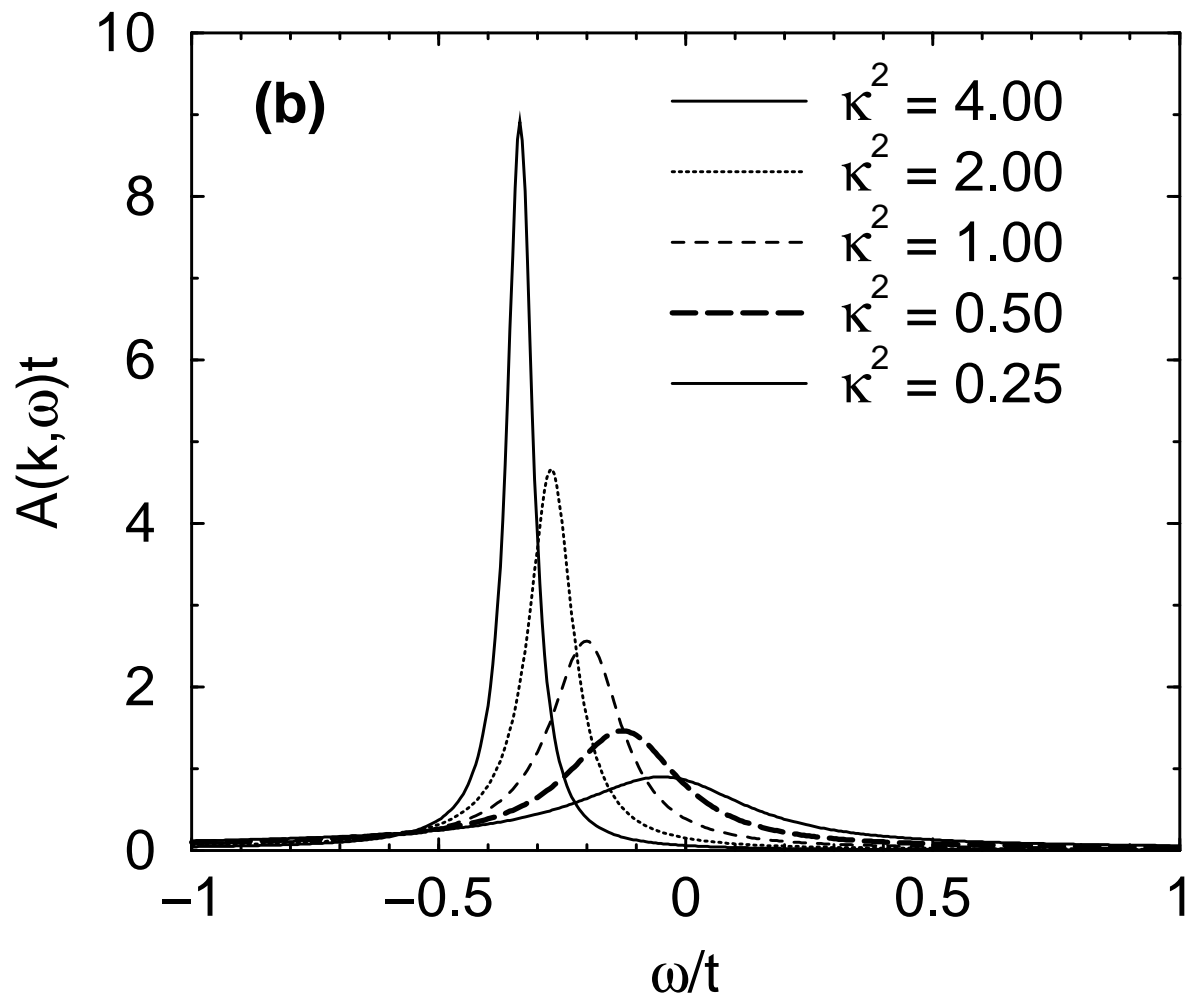


FIG. 1. Diagrammatic expansion for the single particle Green's function. The dashed line connected at one end only to the solid line represents the interaction of the fermions with the dynamical molecular field and the brackets the average over the Gaussian distribution of these fields. The averaging over the distribution of molecular fields is carried out by pairing the dashed lines in all possible ways, each pairing giving a factor proportional to the two-point correlation function of the molecular field, the dynamical susceptibility $\chi(\mathbf{q}, i\nu_n)$ according to Eqs. (2.11,2.12). The lower part of the figure shows the pairings one obtains up to two spin or charge-fluctuation exchanges.

Eliashberg



Eliashberg ; $k = (\pi, \pi/8)$



Eliashberg ; $k = (3\pi/8, 3\pi/8)$

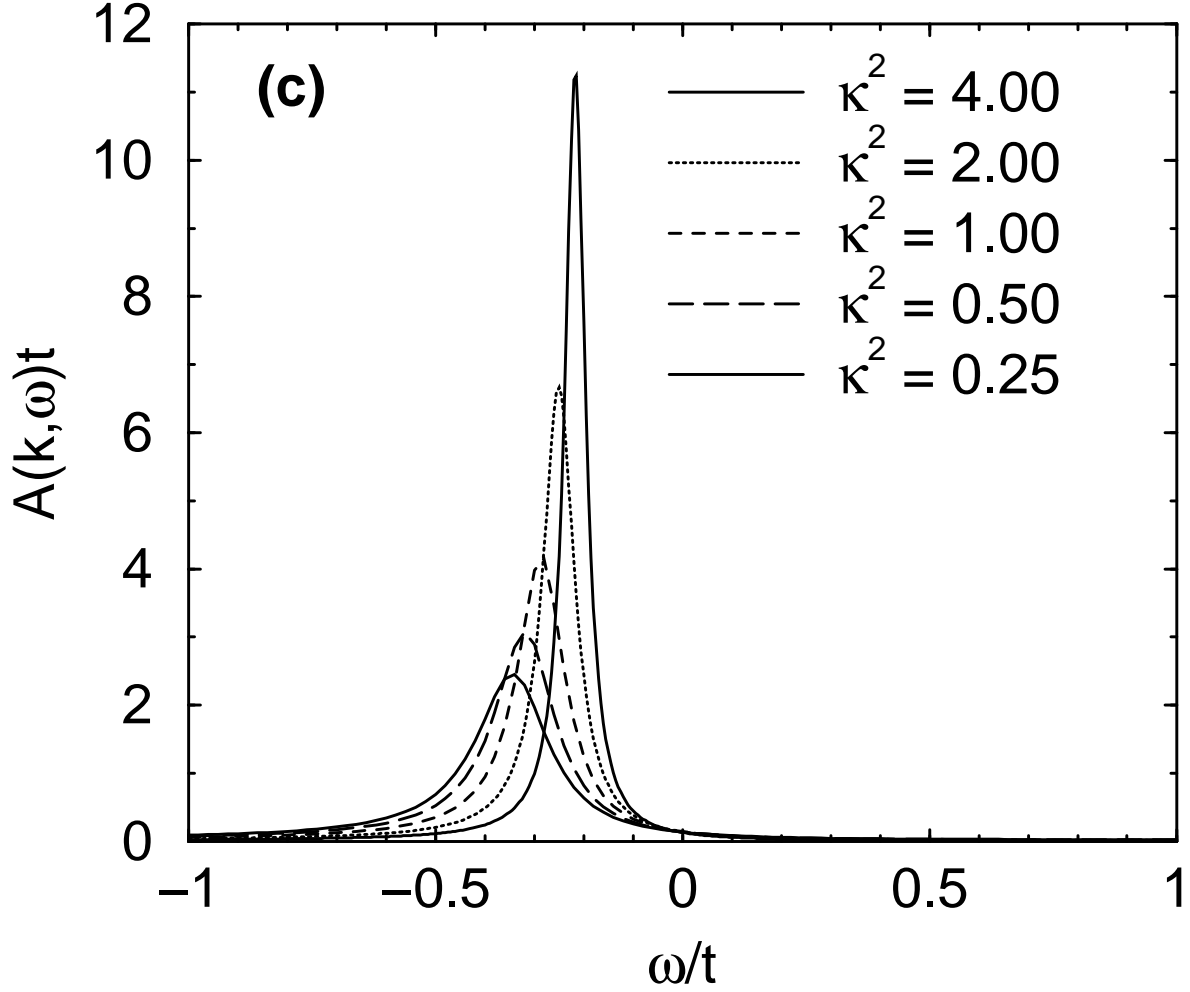
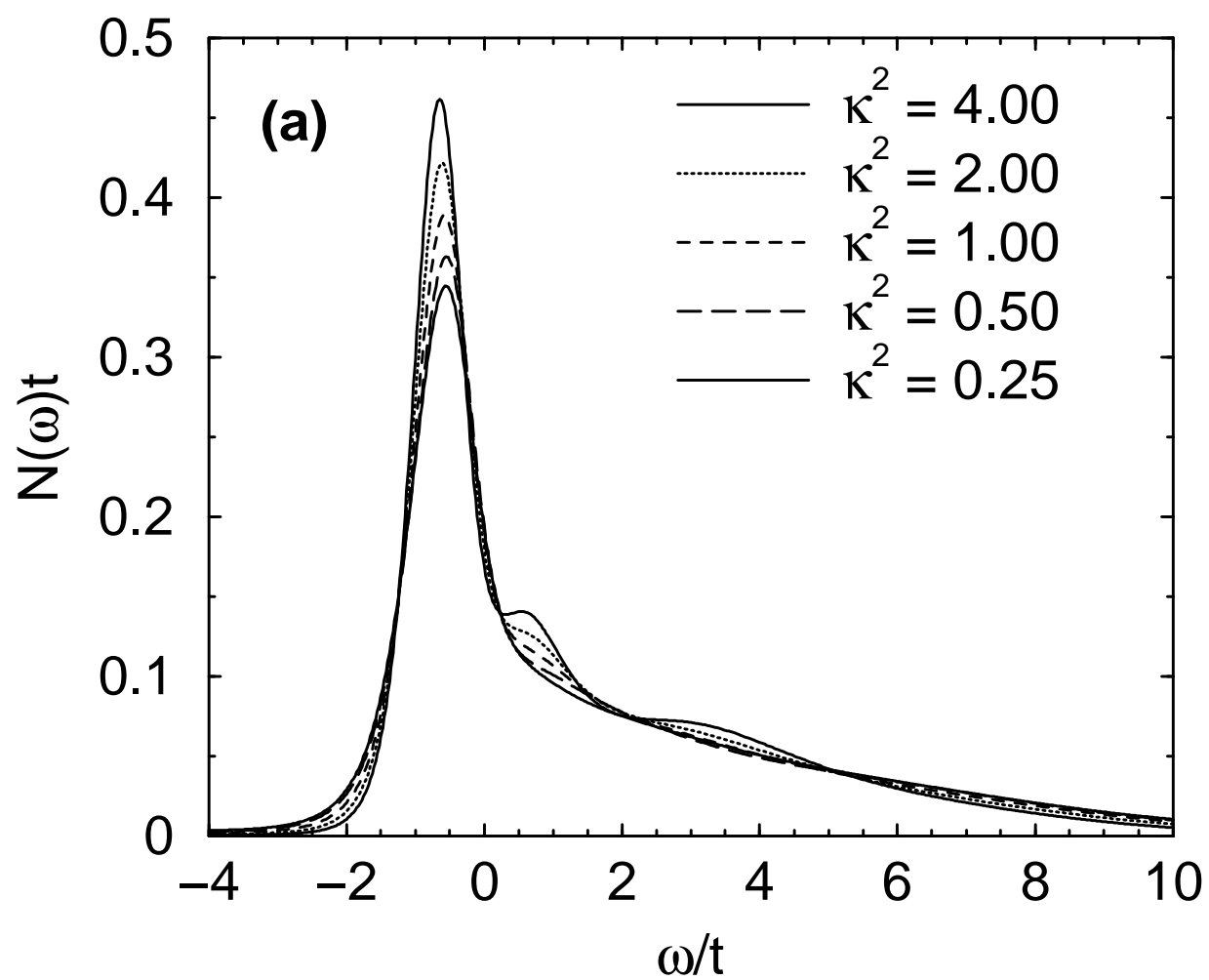
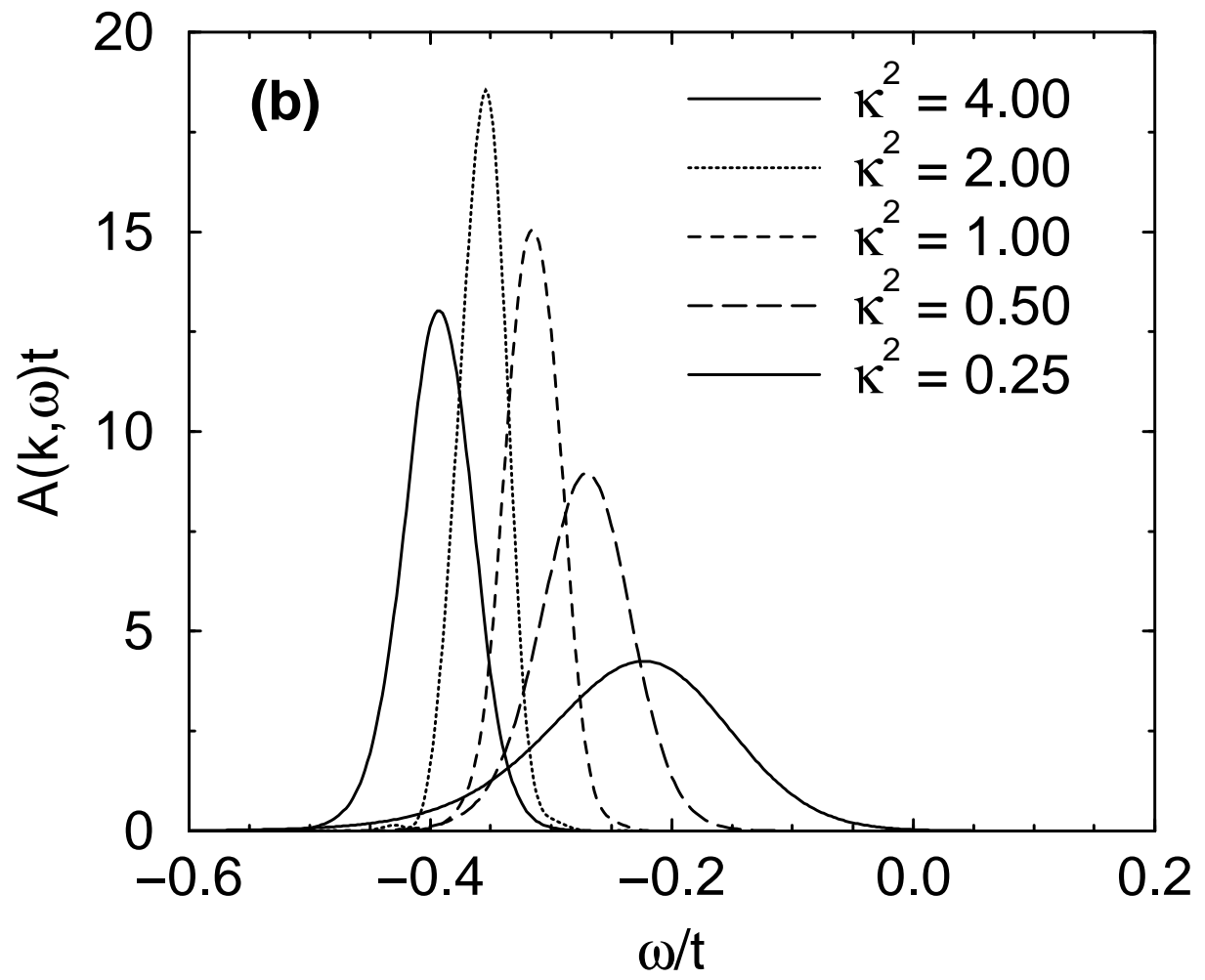


FIG. 2. The one-loop approximation for the quasiparticle properties for both commensurate charge-fluctuations and antiferromagnetic spin-fluctuations. The tunneling density of states $N(\omega)$ is shown in (a) while (b) and (c) show the quasiparticle spectral function $A(\mathbf{k}, \omega)$ for momenta just below the Fermi level. (b) shows $A(\mathbf{k}, \omega)$ for a wavevector close to the Van Hove singularity and (c) shows $A(\mathbf{k}, \omega)$ for a wavevector along the diagonal of the Brillouin zone.

Charge-fluctuations



Charge-fluctuations ; $k = (\pi, \pi/8)$



Charge-fluctuations ; $\mathbf{k} = (3\pi/8, 3\pi/8)$

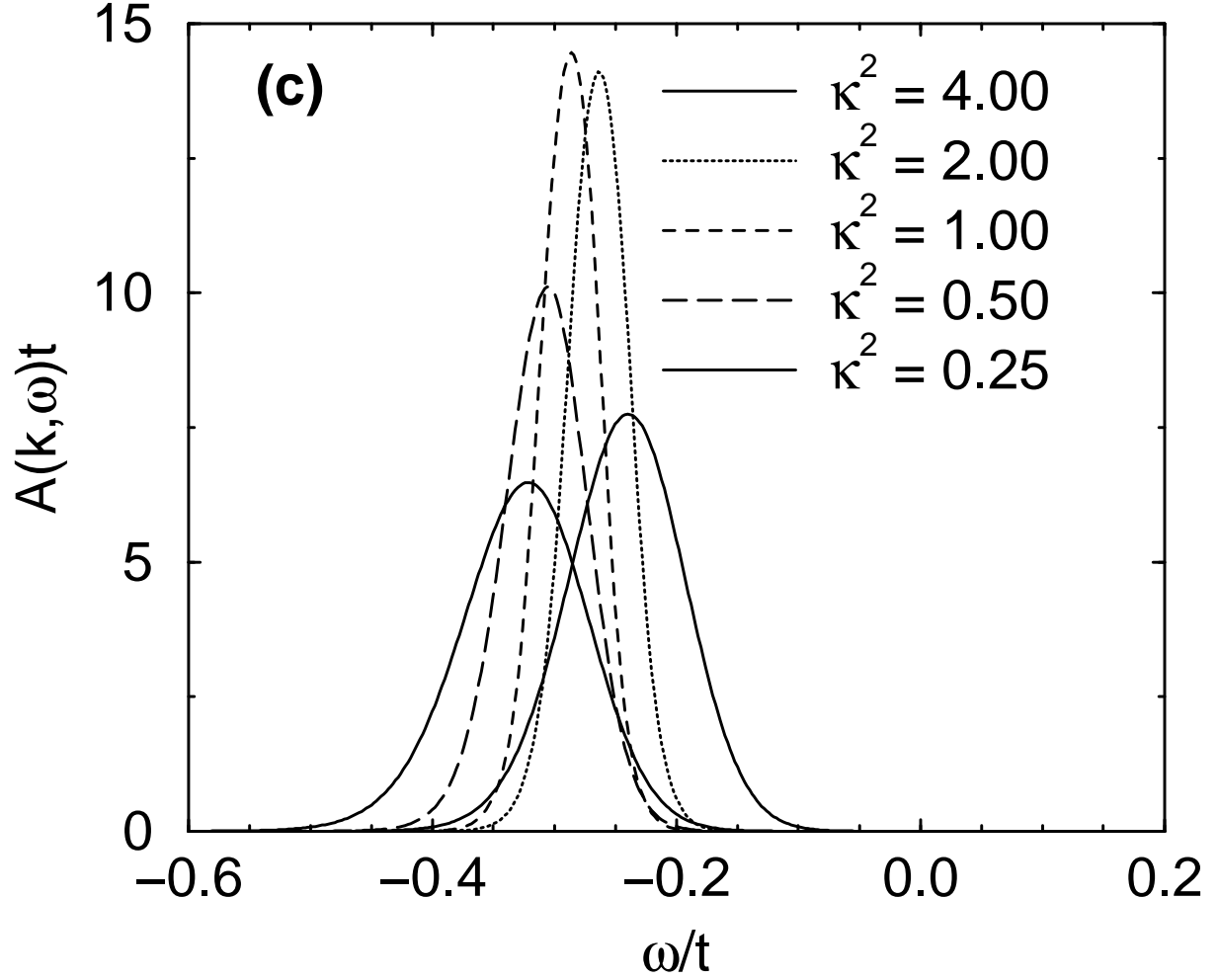
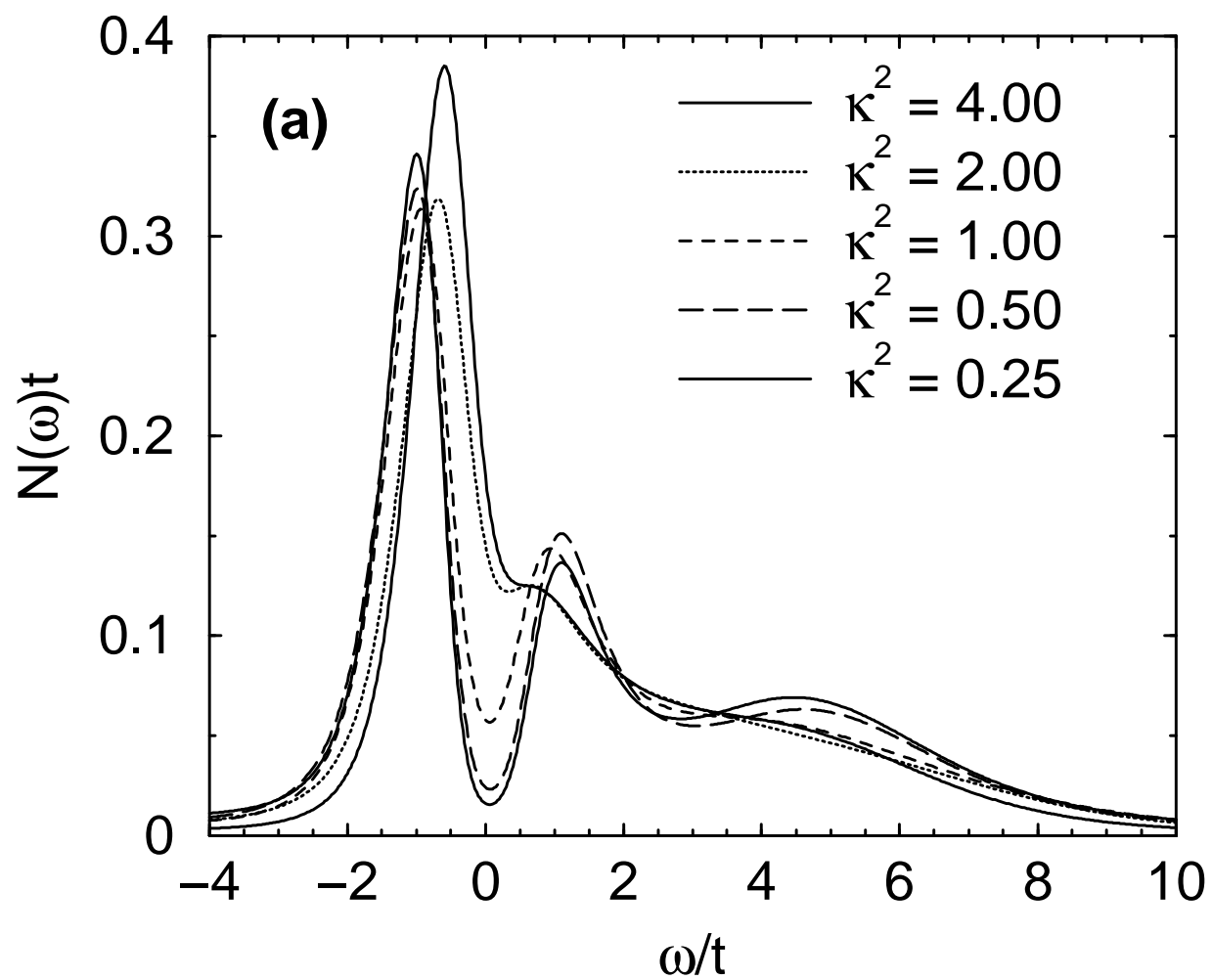
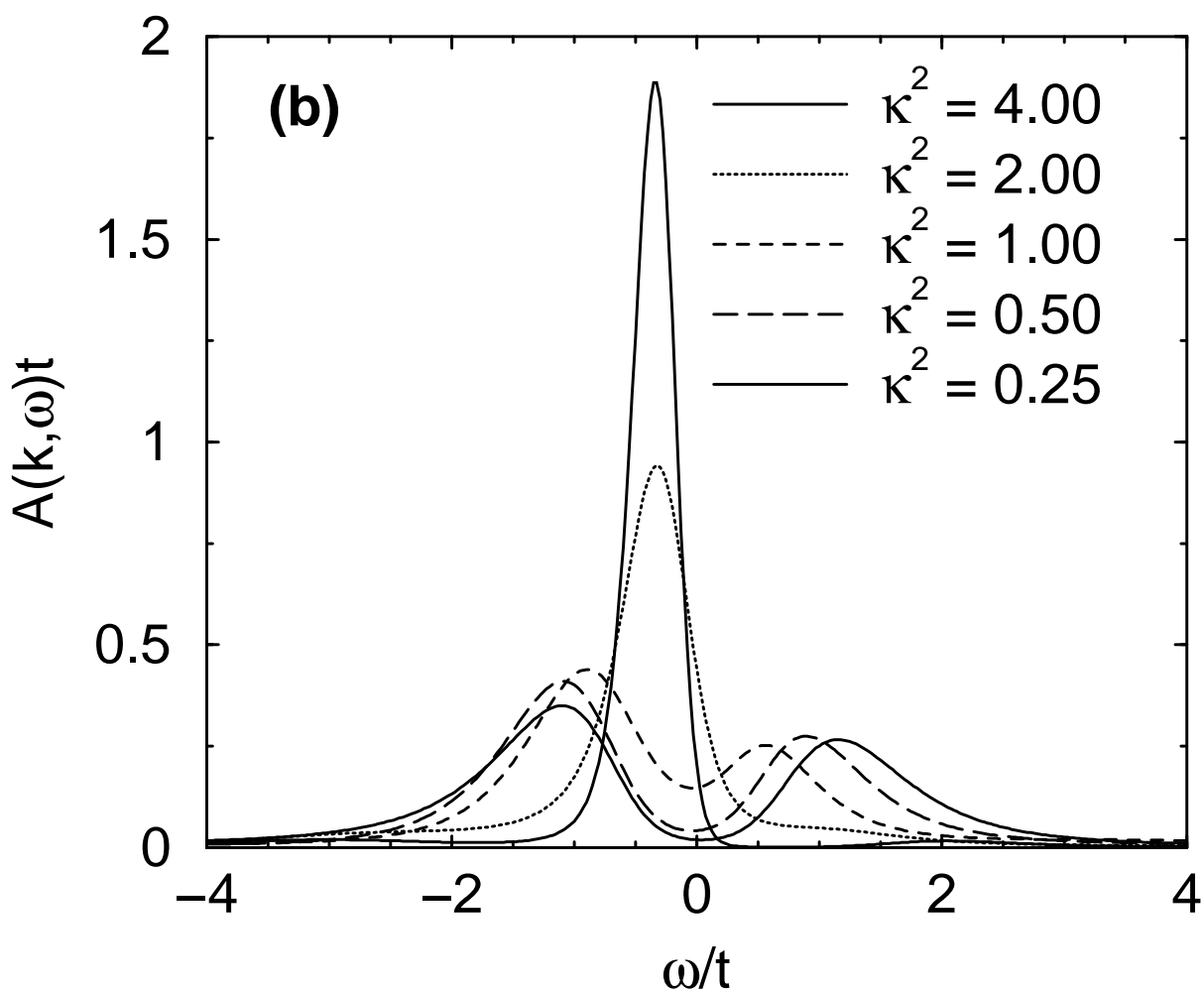


FIG. 3. Quasiparticle properties for a coupling to a scalar dynamical molecular field Φ . The tunneling density of states $N(\omega)$ is shown in (a) while (b) and (c) show the quasiparticle spectral function $A(\mathbf{k}, \omega)$ for momenta just below the Fermi level. (b) shows $A(\mathbf{k}, \omega)$ for a wavevector close to the Van Hove singularity and (c) shows $A(\mathbf{k}, \omega)$ for a wavevector along the diagonal of the Brillouin zone.

AF Spin-fluctuations



AF Spin-fluctuations ; $k = (\pi, \pi/8)$



AF Spin-fluctuations ; $\mathbf{k} = (3\pi/8, 3\pi/8)$

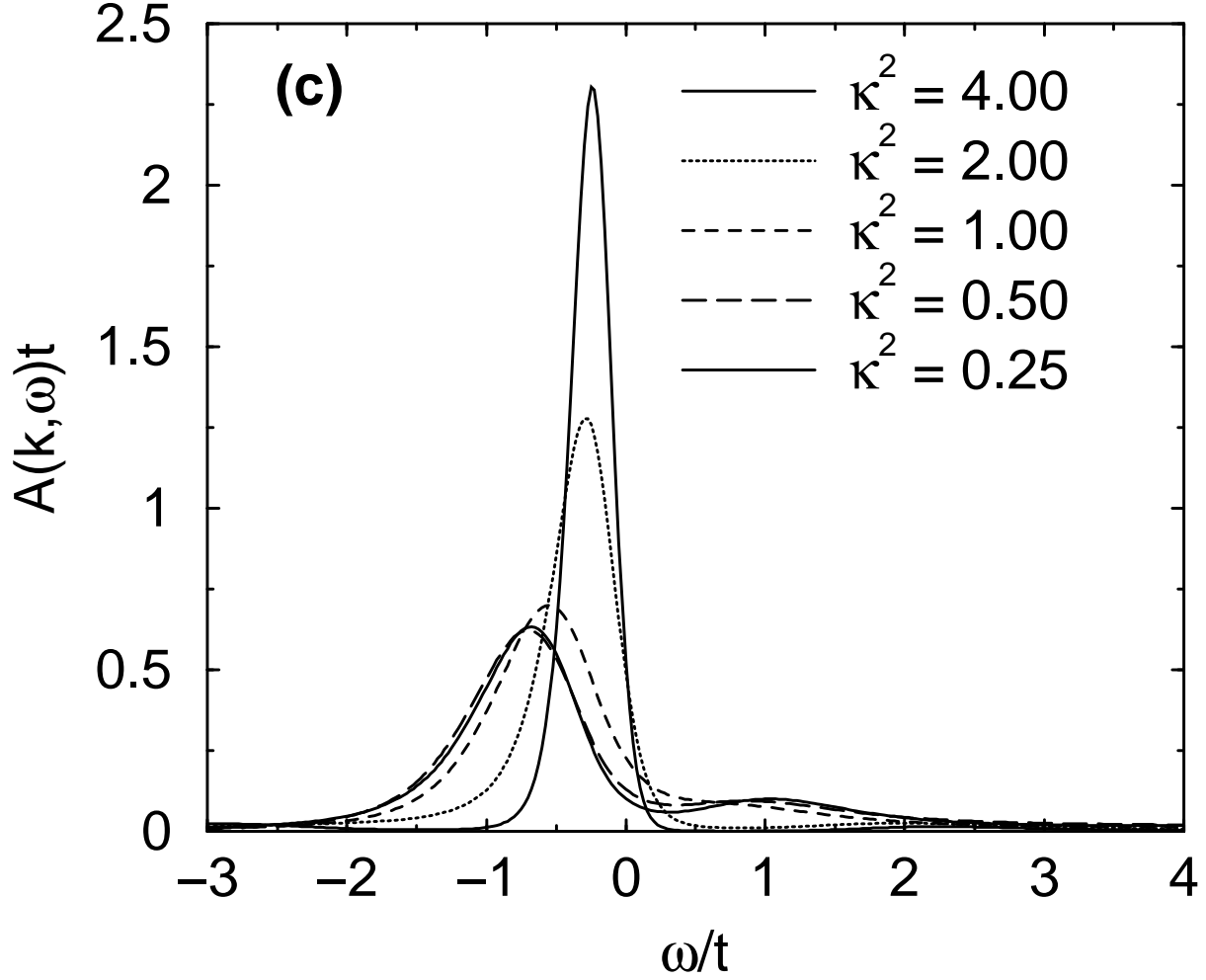
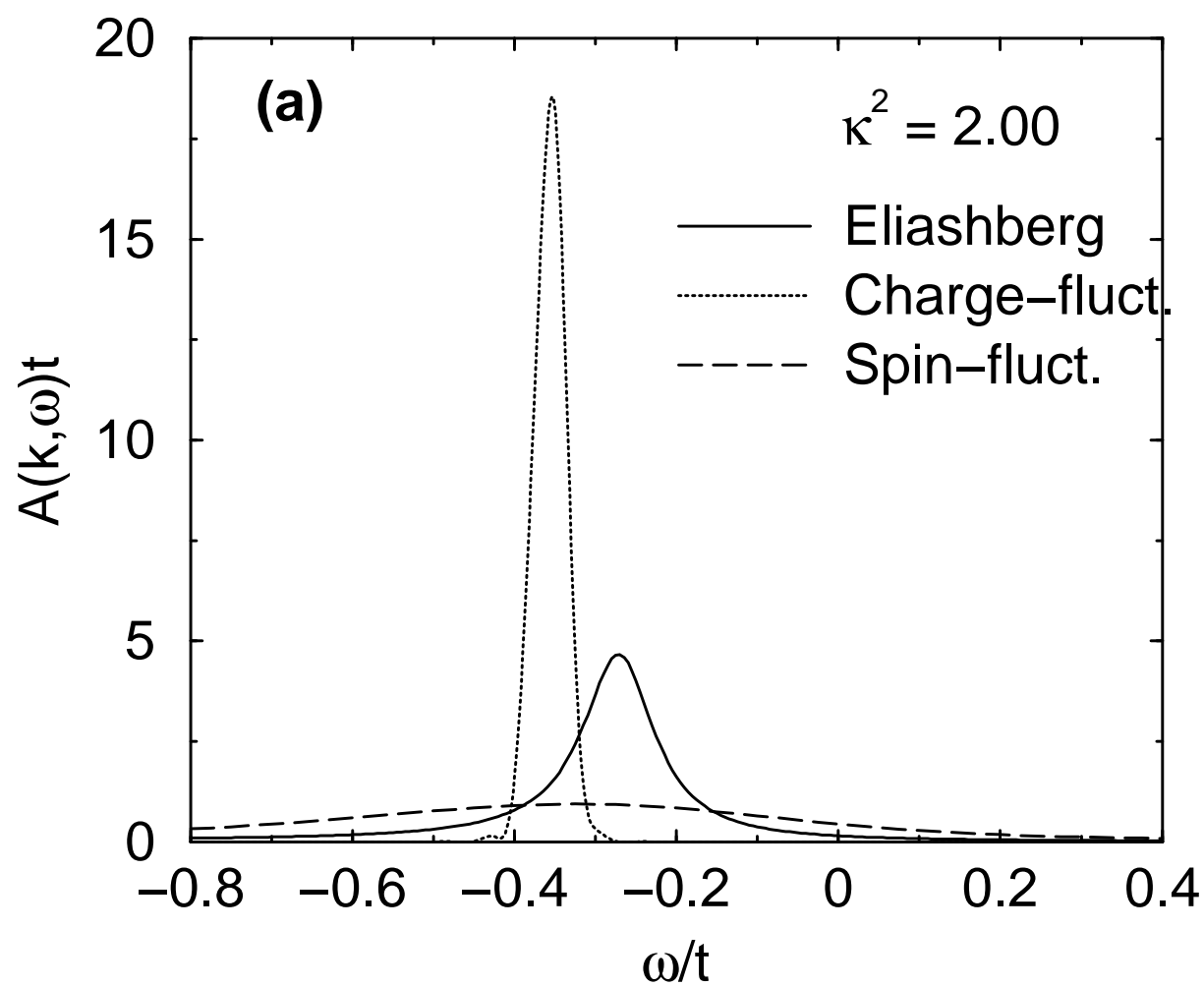


FIG. 4. Quasiparticle properties for a coupling to an exchange vector dynamical molecular field \mathbf{M} with antiferromagnetic correlations. The tunneling density of states $N(\omega)$ is shown in (a) while (b) and (c) show the quasiparticle spectral function $A(\mathbf{k}, \omega)$ for momenta just below the Fermi level. (b) shows $A(\mathbf{k}, \omega)$ for a wavevector close to the Van Hove singularity and (c) shows $A(\mathbf{k}, \omega)$ for a wavevector along the diagonal of the Brillouin zone.

$$\mathbf{k} = (\pi, \pi/8)$$



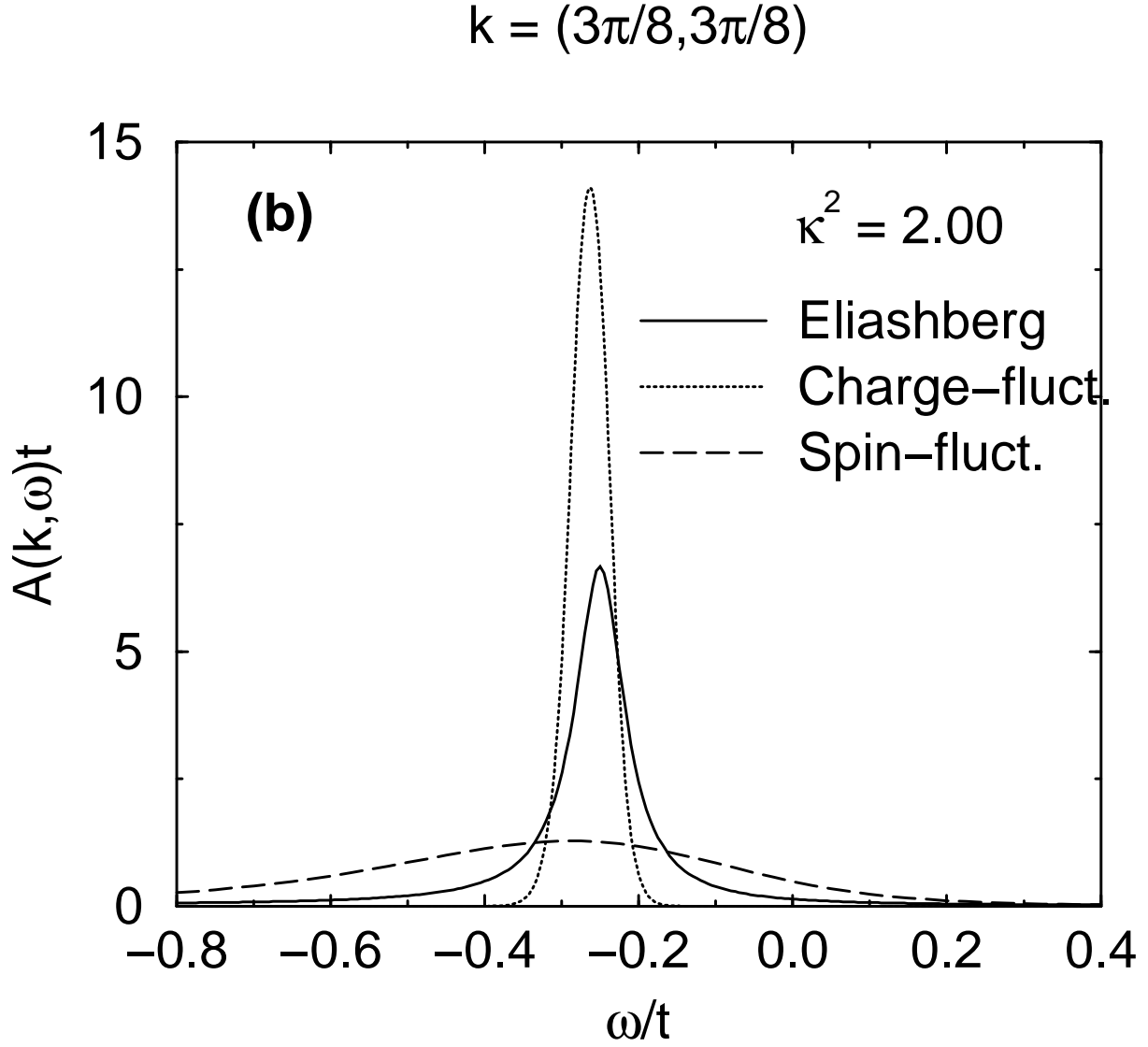
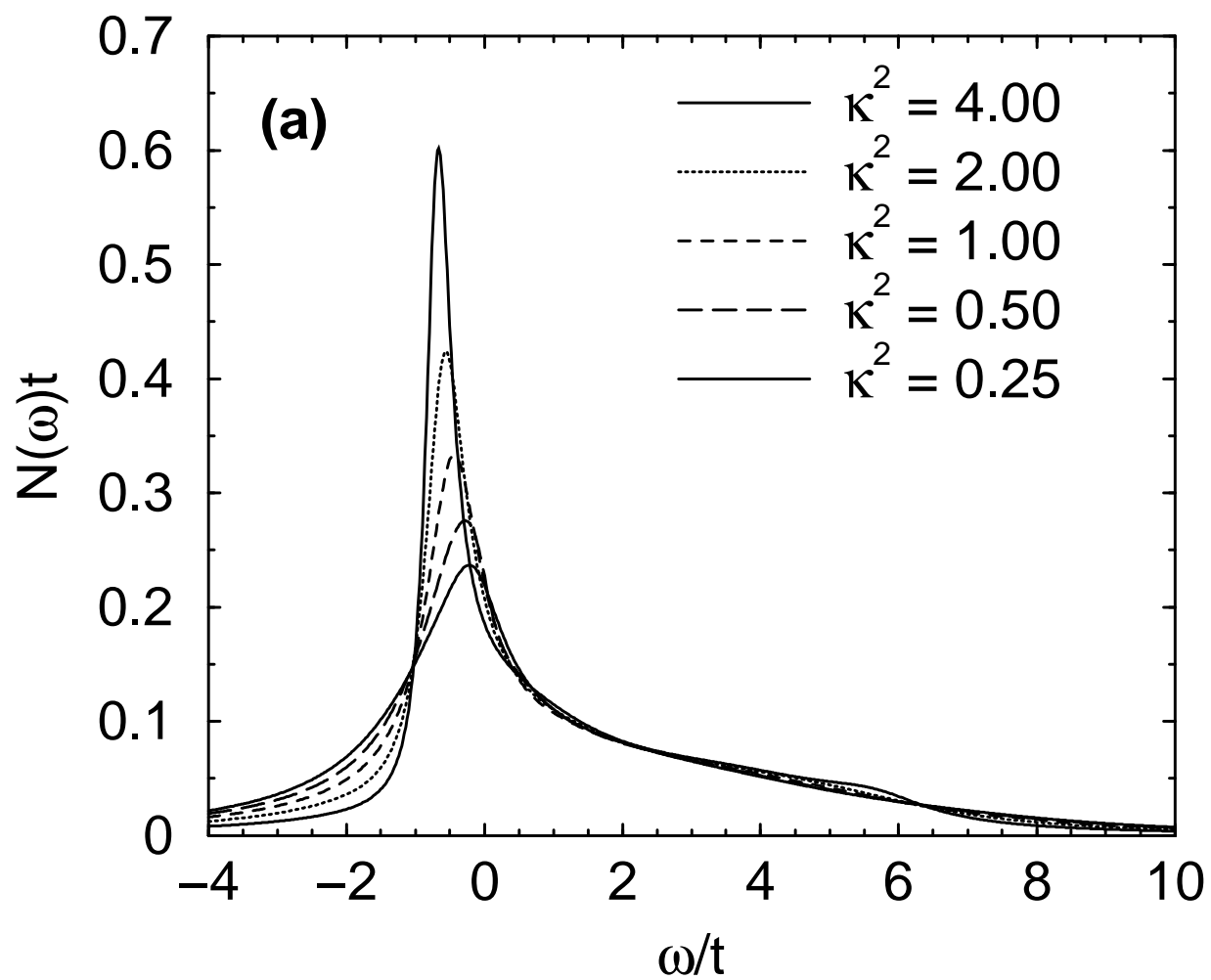
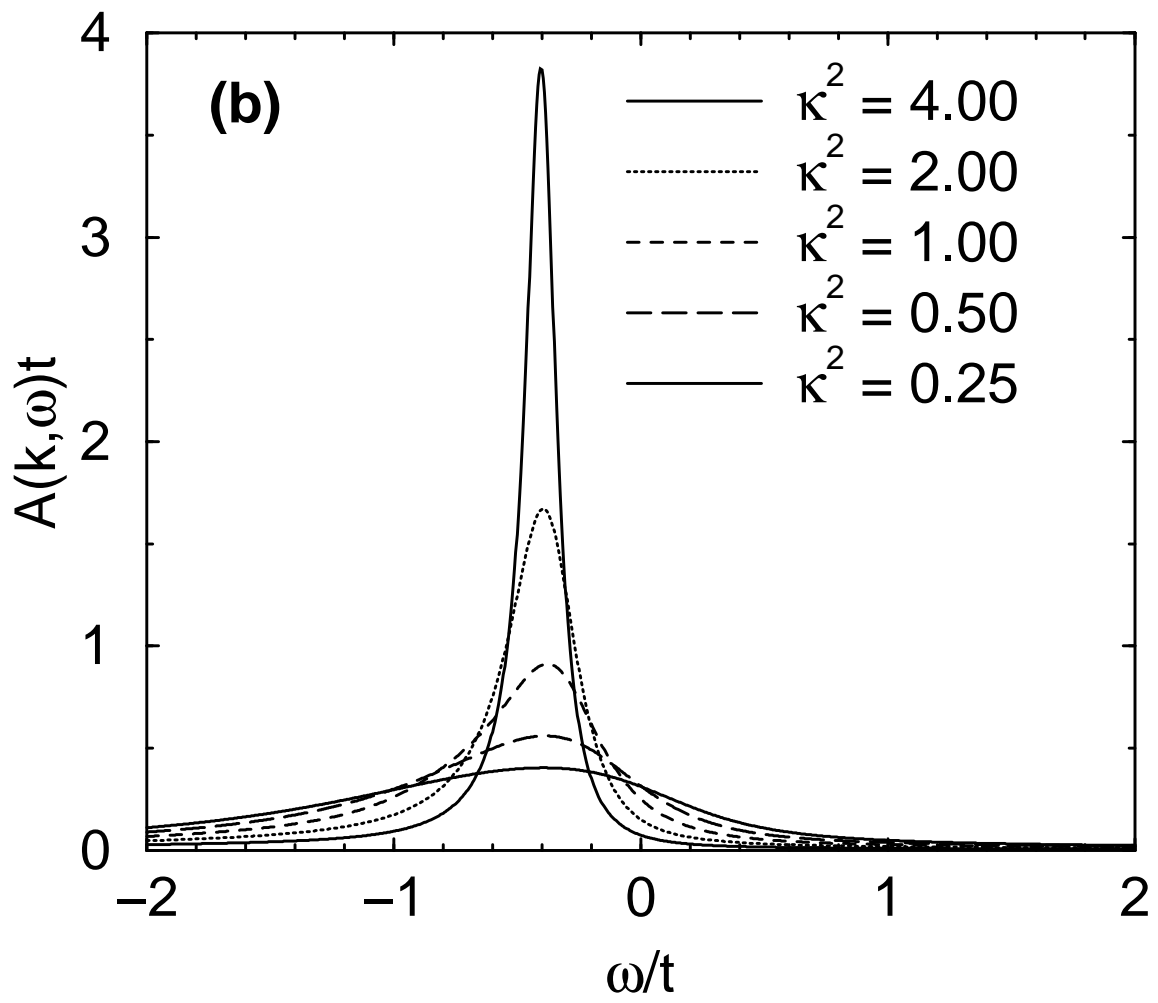


FIG. 5. Comparison of the one-loop self-consistent versus the non-perturbative calculation of charge- and spin-fluctuation exchanges. (a) shows the spectral function $A(\mathbf{k}, \omega)$ for a wavevector close to the Van-Hove singularity and (b) shows $A(\mathbf{k}, \omega)$ for a wavevector along the diagonal of the Brillouin zone.

Eliashberg



Eliashberg ; $k = (\pi, \pi/8)$



Eliashberg ; $k = (3\pi/8, 3\pi/8)$

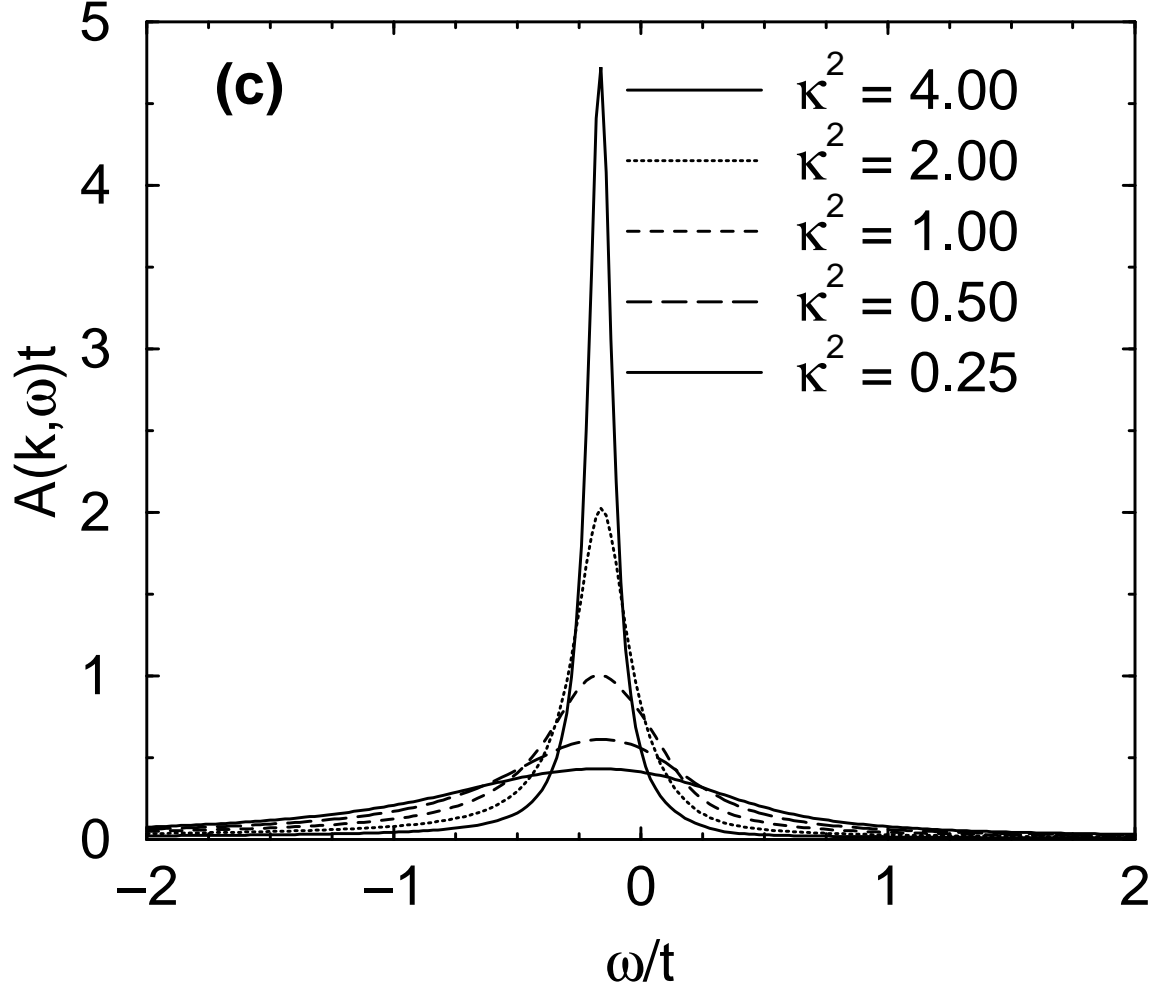
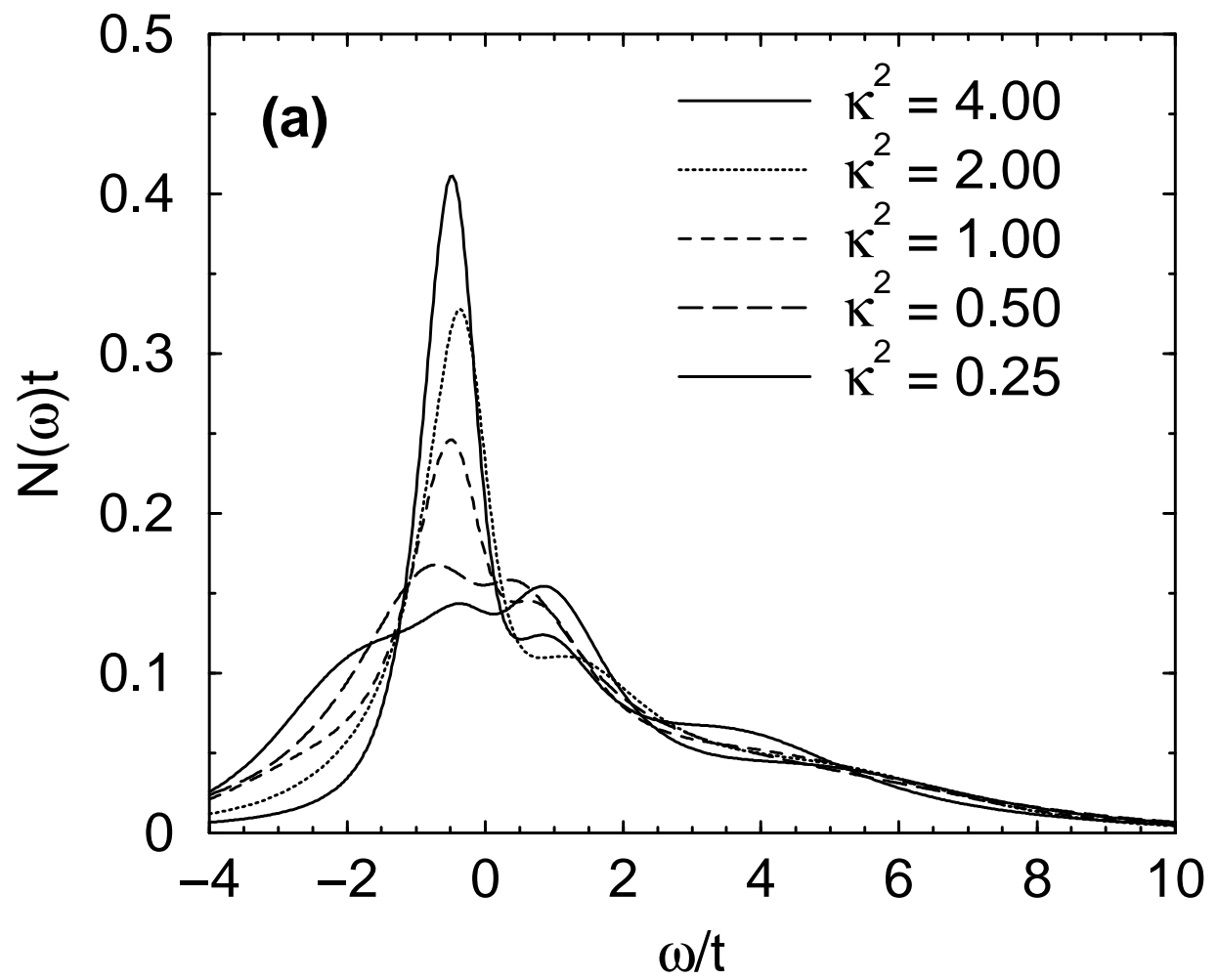
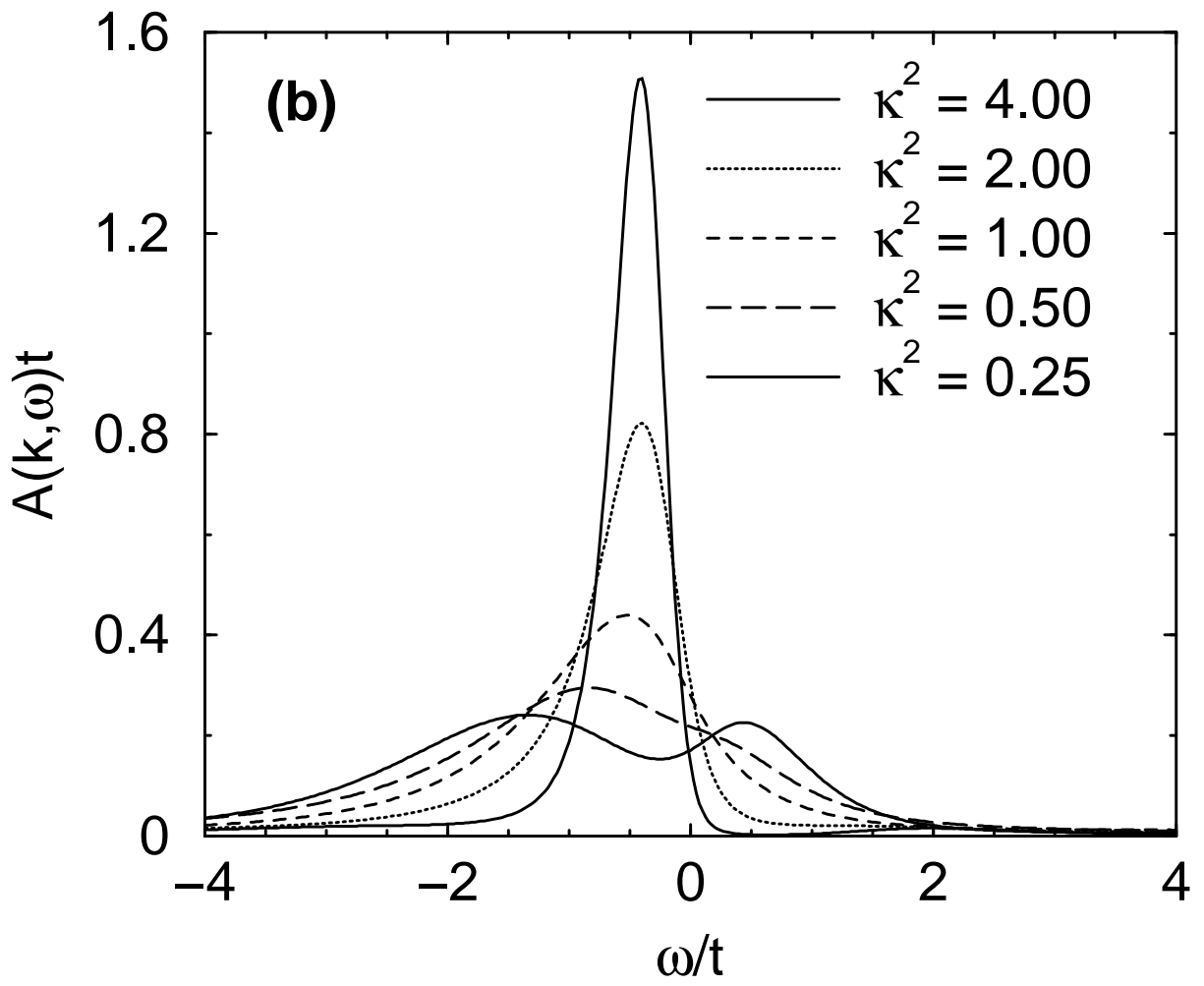


FIG. 6. The one-loop approximation for the quasiparticle properties for ferromagnetic spin-fluctuations. The tunneling density of states $N(\omega)$ is shown in (a) while (b) and (c) show the quasiparticle spectral function $A(\mathbf{k}, \omega)$ for momenta just below the Fermi level. (b) shows $A(\mathbf{k}, \omega)$ for a wavevector close to the Van Hove singularity and (c) shows $A(\mathbf{k}, \omega)$ for a wavevector along the diagonal of the Brillouin zone.

FE Spin-fluctuations



FE Spin-fluctuations ; $k = (\pi, \pi/8)$



FE Spin-fluctuations ; $\mathbf{k} = (3\pi/8, 3\pi/8)$

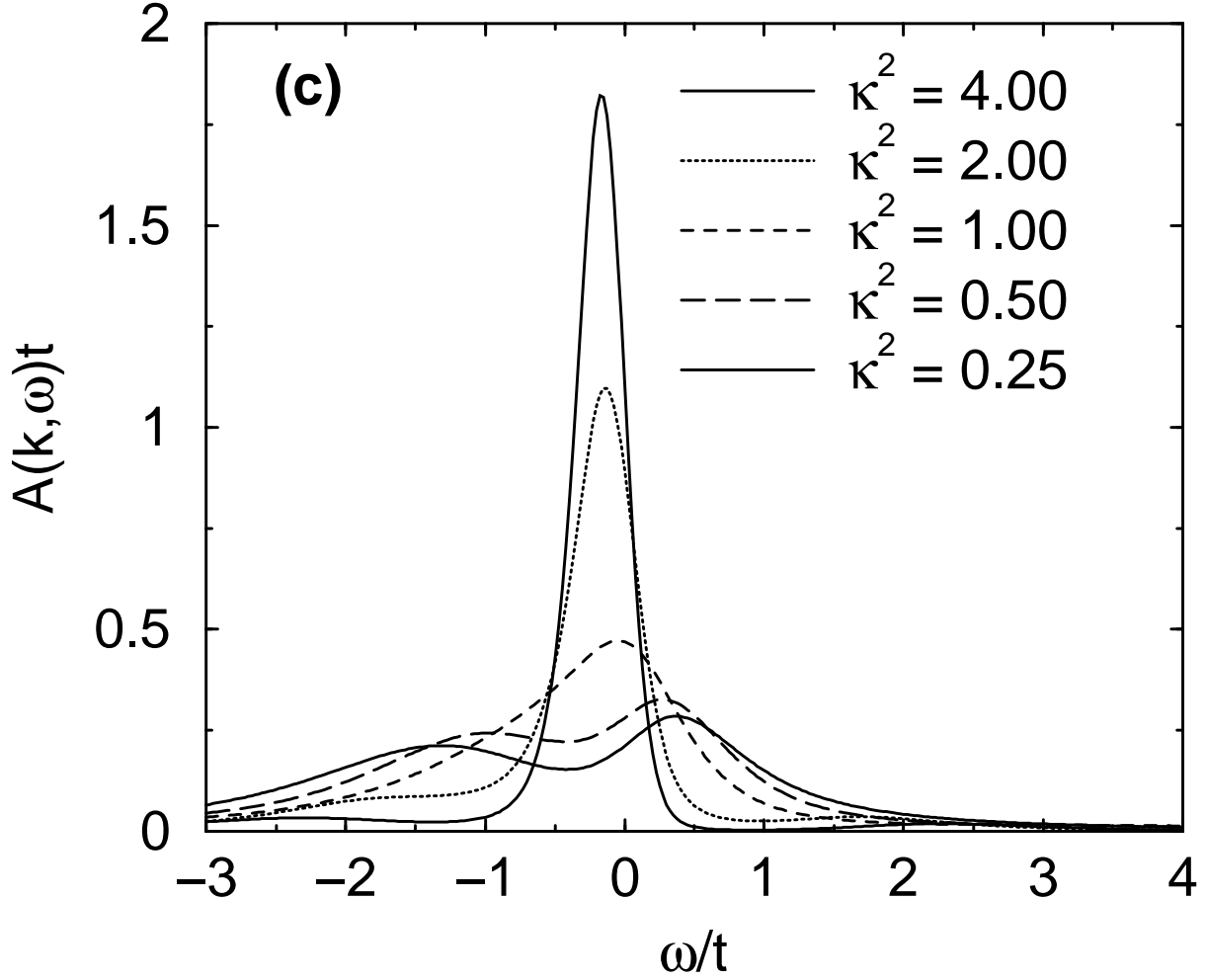


FIG. 7. Quasiparticle properties for a coupling to an exchange vector dynamical molecular field \mathbf{M} with ferromagnetic correlations. The tunneling density of states $N(\omega)$ is shown in (a) while (b) and (c) show the quasiparticle spectral function $A(\mathbf{k}, \omega)$ for momenta just below the Fermi level. (b) shows $A(\mathbf{k}, \omega)$ for a wavevector close to the Van Hove singularity and (c) shows $A(\mathbf{k}, \omega)$ for a wavevector along the diagonal of the Brillouin zone.

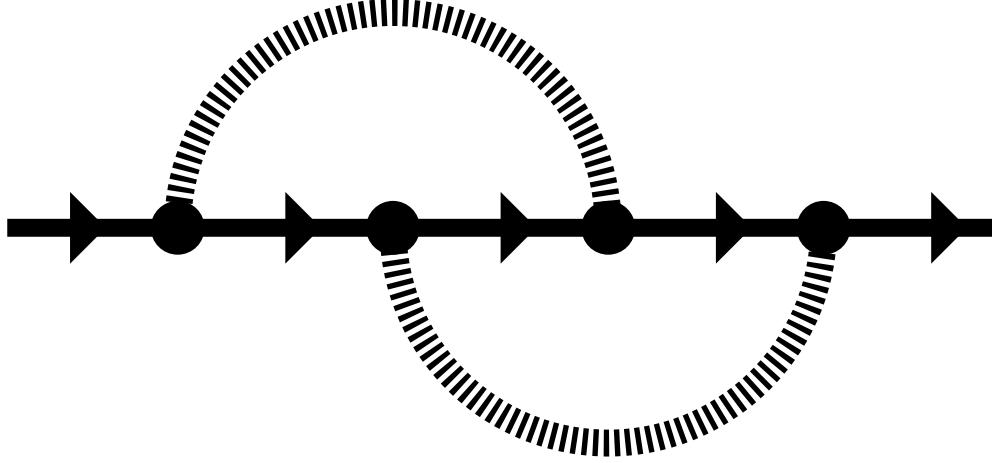
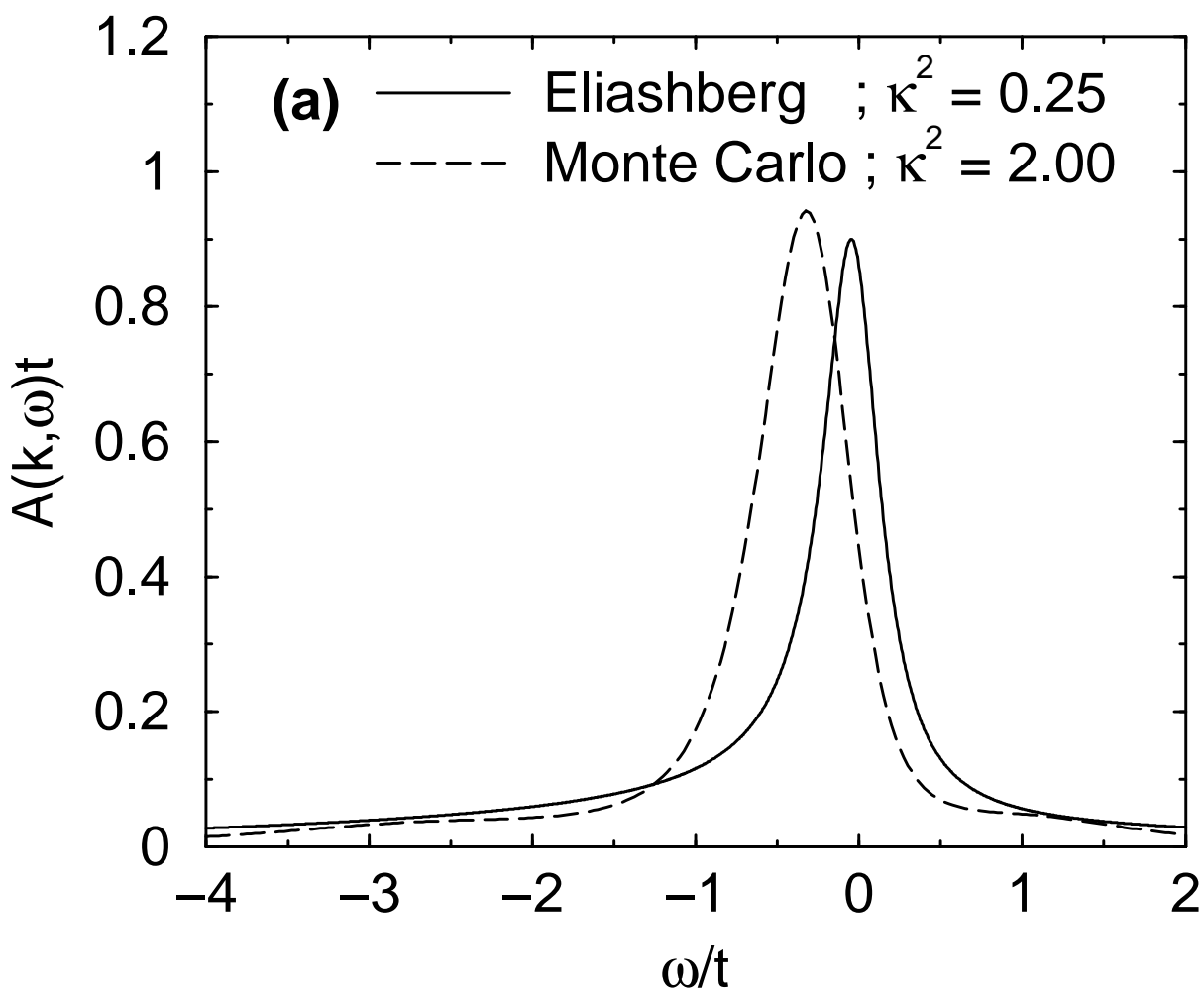


FIG. 8. First order vertex correction to the one-loop self-energy. The way spin is carried through the diagram depends on the kind of molecular field. A Pauli matrix is associated with each vertex in the case of a coupling of quasiparticles to magnetic fluctuations. In the case of exchange of charge fluctuations, each vertex simply carries a unit matrix, namely the spin orientation is unchanged at each vertex of the diagram.

$$\mathbf{k} = (\pi, \pi/8)$$



$$\mathbf{k} = (3\pi/8, 3\pi/8)$$

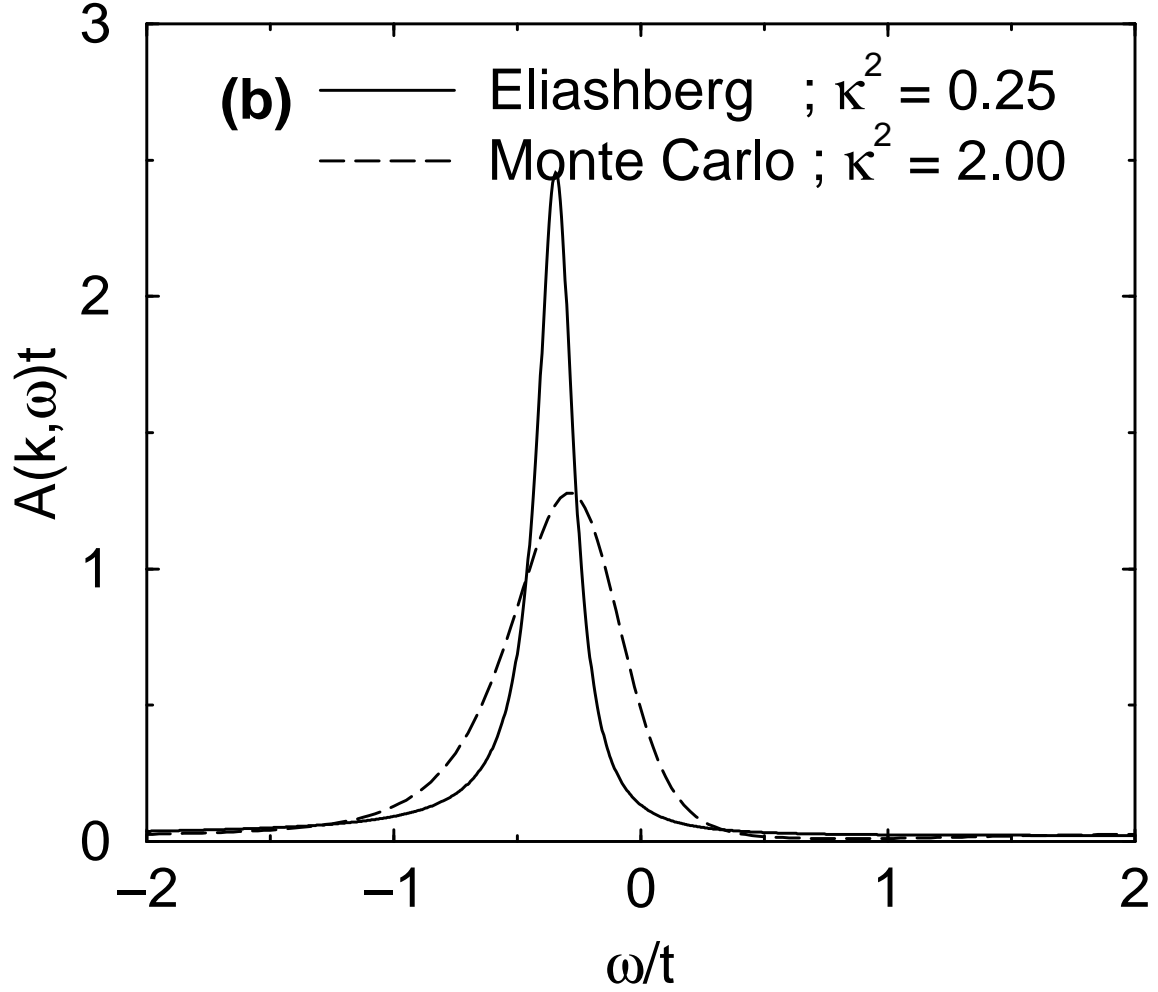
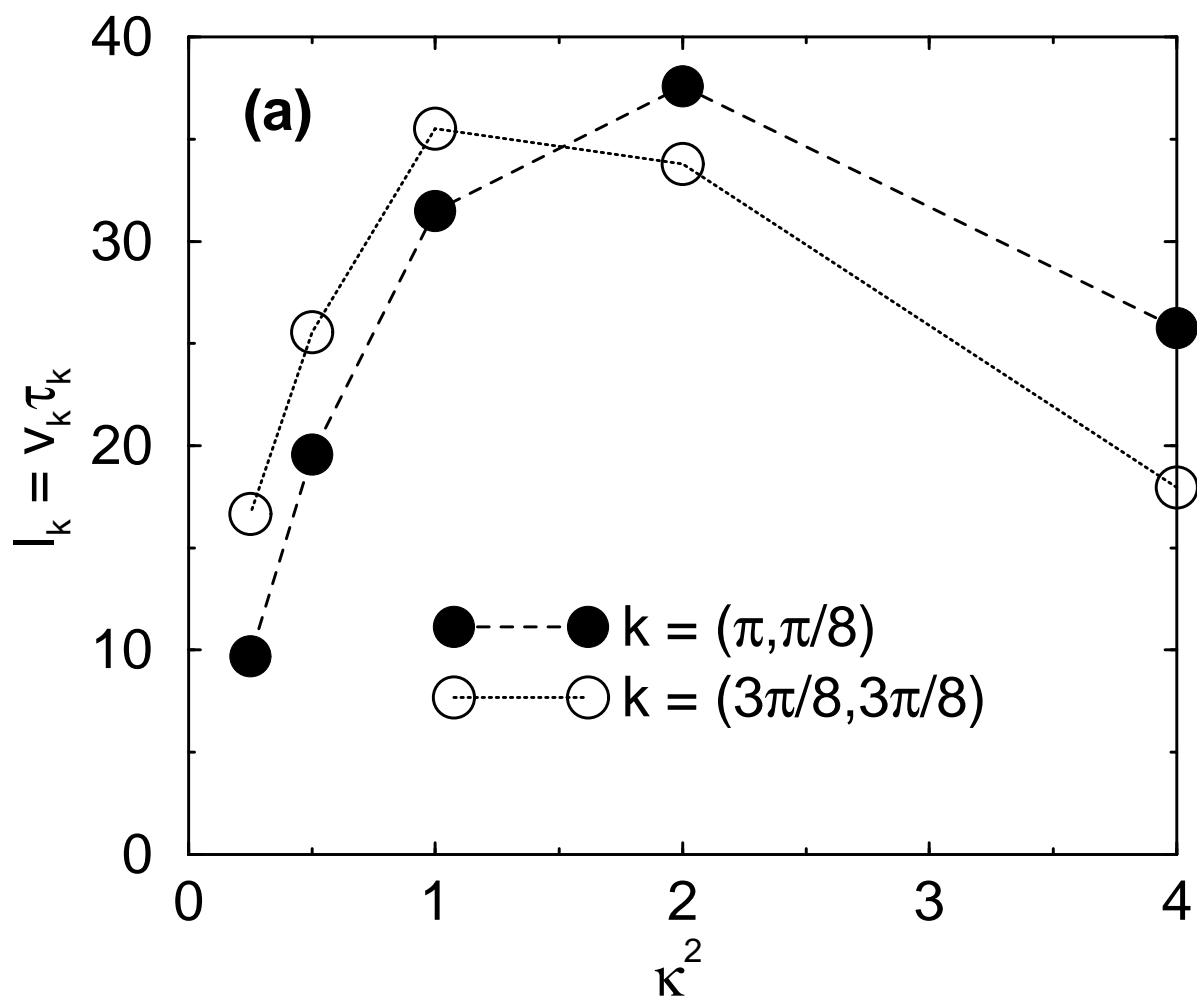
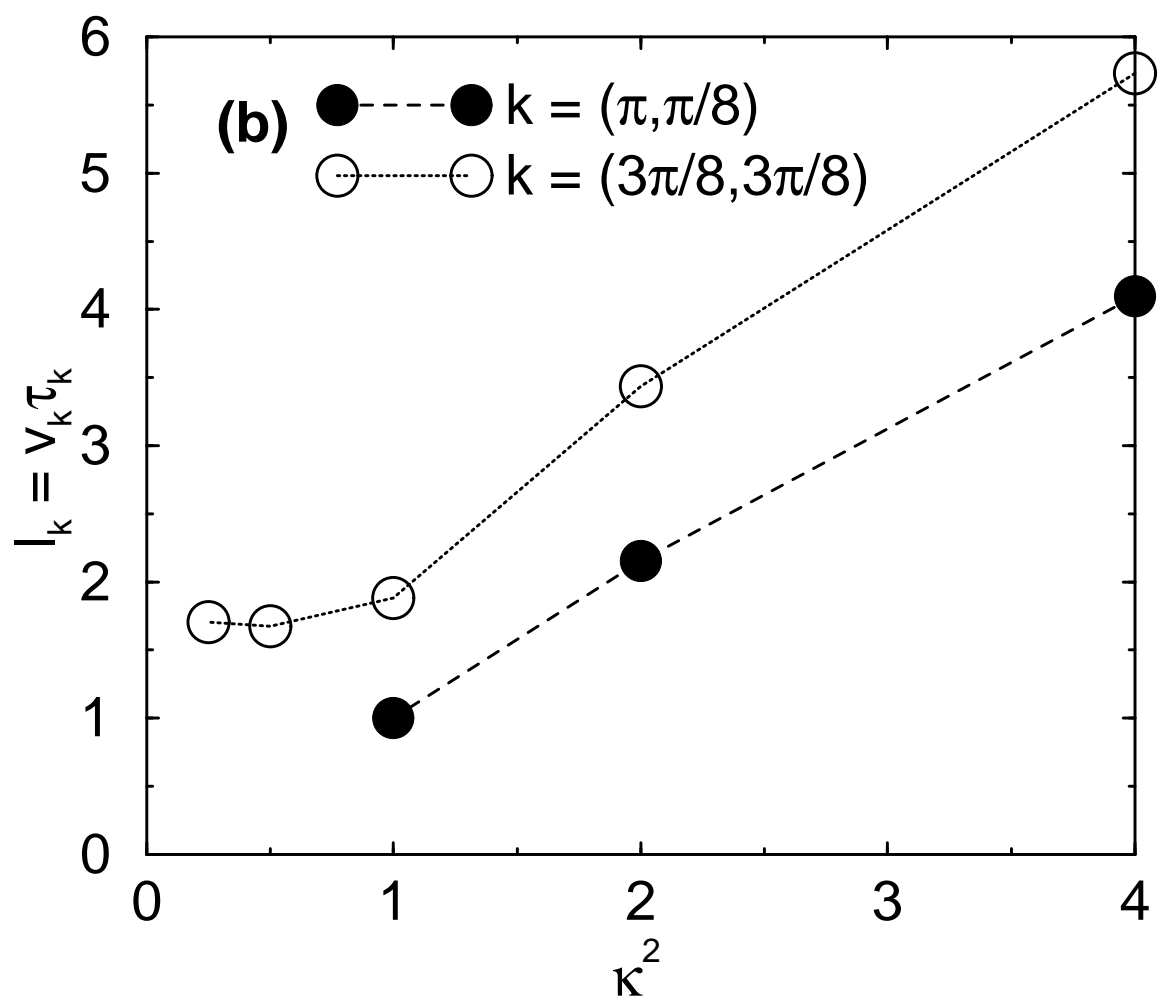


FIG. 9. Comparison of the single antiferromagnetic spin-fluctuation exchange approximation for the quasiparticle spectral function with a renormalized correlation wavevector $\kappa_{eff}^2 = 0.35$ and the non-perturbative result with $\kappa^2 = 2$. In both cases the dimensionless coupling constant $g^2\chi_0/t = 2$. (a) and (b) show the quasiparticle spectral function $A(\mathbf{k}, \omega)$ for momenta just below the Fermi level. (a) shows $A(\mathbf{k}, \omega)$ for a wavevector close to the Van Hove singularity and (b) shows $A(\mathbf{k}, \omega)$ for a wavevector along the diagonal of the Brillouin zone.

Charge-fluctuations



AF Spin-fluctuations



FE Spin-fluctuations

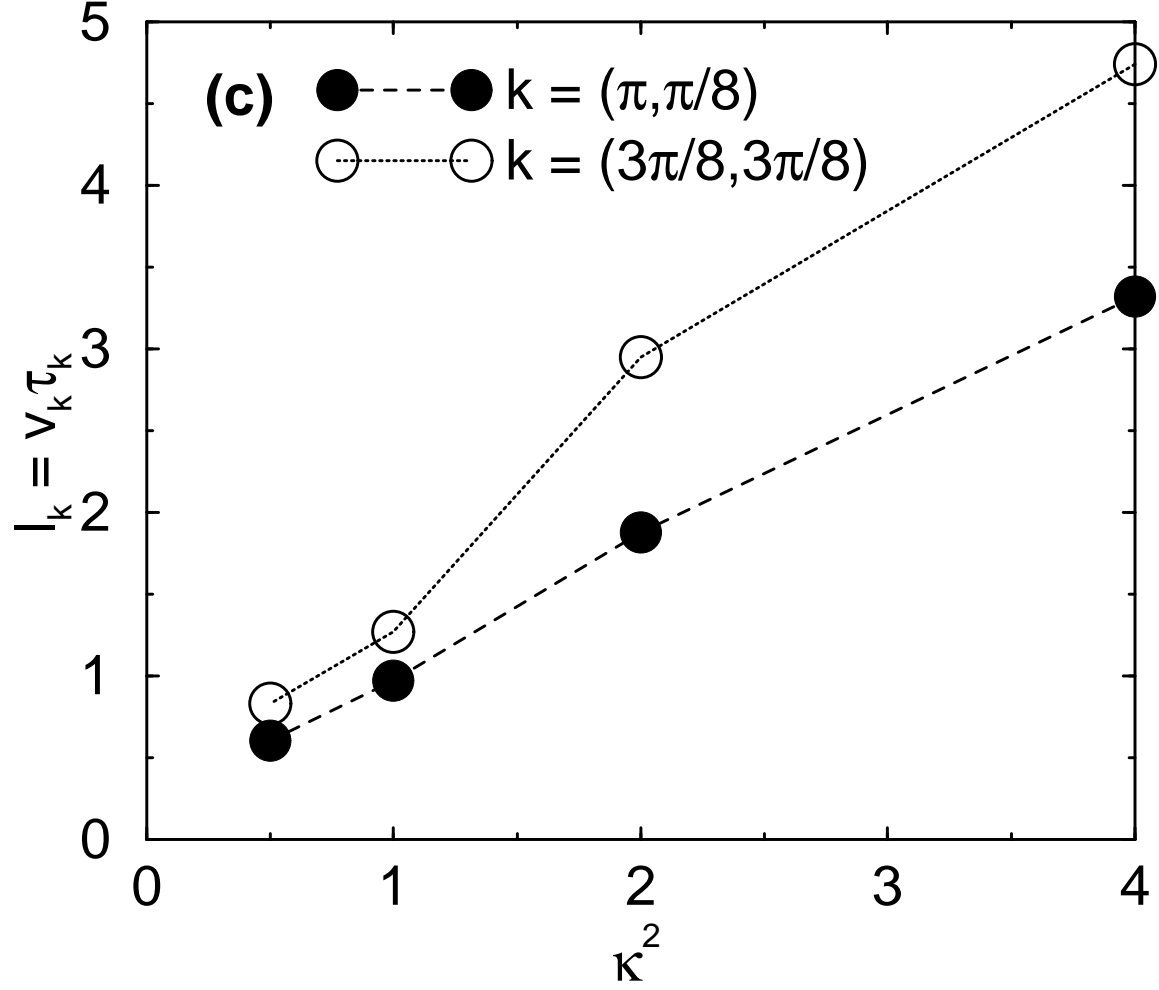


FIG. 10. Approximate quasiparticle mean-free paths $l_{\mathbf{k}}$ for $\mathbf{k} = (\pi, \pi/8)$ and $\mathbf{k} = (3\pi/8, 3\pi/8)$ obtained from Lorentzian fits to the numerical results for the spectral function. (a) shows $l_{\mathbf{k}}$ for coupling to charge-fluctuations, (b) to antiferromagnetic spin-fluctuations and (c) to ferromagnetic spin-fluctuations.